ECMWF COPERNICUS REPORT

Copernicus Climate Change

Differences between CMIP5 GCMs downscaled by EURO-CORDEX RCMs and the full CMIP5 and CMIP6 ensembles, with focus on Europe

Issued by: SMHI / Erik Kjellström

Date: 29/06/2021

Ref: C3S_D34b_Lot2.3.4.2_202106_GCMsDownscaledEUROCORDEX_RCMs_v3

Official reference number service contract: 2017/C3S_34b_Lot2_SMHI/SC4

Contributors

GErics
Katharina Bülow
Ludwig Lierhammer
Claas Teichmann

SMHI
Erik Kjellström

ETH Zürich
Marie-Estelle Demory

Table of Contents

Executive summary

A very large ensemble of more than 130 regional climate simulations for Europe is finalized for the climate change scenarios RCP2.6, RCP4.5 and RCP8.5 (downscaling the CMIP5 GCMs). These simulations constitute a major contribution to the scientific basis on future climate change in Europe, which is needed for impact studies and for taking appropriate adaptation measures.

Now the first publications on the new CMIP6 simulations and the data itself are available. This circumstance makes it very important to compare the different ensembles: the well-established CMIP5 ensemble including the subset of CMIP5 GCMs used as forcing for the EURO-CORDEX RCMs can now be compared with the newer CMIP6 models. Here, we present such an analysis to give the users of the EURO-CORDEX ensemble an idea about how these particular forcing CMIP5 GCMs represent for Europe: i) the full spread of the whole CMIP5 ensemble, ii) how these results reflect the range of the new CMIP6 ensemble and iii) how the CMIP5 and CMIP6 ensembles compare with each other. The EURO-CORDEX RCM ensemble is not evaluated here.

The 30-year mean annual and seasonal mean temperature and precipitation are calculated for the historical period 1981-2010 and two future time slices 2036-2065 and 2070-2099 and averaged over three regions: Northern Europe (NEU), Western & Central Europe (WCE) and the Mediterranean (MED). The model results of the CMIP5 and CMIP6 ensembles are evaluated for the historical time period by comparing them to ERA5 reanalysis data. The projected climate change results for the future are compared between the CMIP5 results for scenario RCP2.6, RCP4.5, RCP8.5 with their corresponding, but not identical, scenarios of CMIP6 SSP1-2.6, SSP2-4.5, SSP5-8.5.

The spread of the annual mean temperature bias is smaller for CMIP6 than for its precursor CMIP5 in Northern Europe (NEU) and Western & Central Europe (WCE), but larger in the Mediterranean (MED). Individual CMIP6 models still show strong temperature and precipitation biases.

This study confirms the previous finding for temperature and precipitation change at the end of the 21st century in Europe. Regional and seasonal features of temperature and precipitation changes in Europe exist in the results of the CMIP5 and CMIP6 ensemble. These include: a distinct precipitation and temperature increase during winter in Northern Europe; and a pronounced drying in the Mediterranean during summer in RCP85/SSP585. The median and interquartile spread of the temperature change of each scenario from CMIP6 is higher than its corresponding scenario in CMIP5. In Northern and Western & Central Europe, the median of the precipitation change is more pronounced in CMIP6 than in CMIP5: during winter it is slightly higher and lower during summer. The CMIP5 models used as forcing for EURO-CORDEX RCMs cover half of the full spread of the temperature and precipitation change of the CMIP5 ensemble in Western & Central Europe and the Mediterranean. For Northern Europe, the spread is even less well represented.

Introduction

A very large ensemble of more than 130 EURO-CORDEX regional climate simulations for Europe is finalized for the climate change scenarios RCP2.6, RCP4.5 and RCP8.5. These simulations constitute a major contribution to the scientific basis on future climate change in Europe, which is needed for impact studies and for taking appropriate adaptation measures. This EURO-CORDEX ensemble is a combination of 11 regional climate models (RCMs) forced by mainly 8 different global climate models (GCMs). These forcing GCMs are part of the CMIP5 (Fifth phase of the Climate Model Intercomparison Project) GCM ensemble. Now the first publications on the new CMIP6 simulations and the data itself from these simulations are available. This circumstance makes it important to compare the different ensembles: CMIP5, CMIP5 used as forcing for EURO-CORDEX RCMs, and CMIP6 with each other. To give the users of the EURO-CORDEX ensemble an idea, how these particular forcing GCMs represent the full spread of the whole CMIP5 ensemble and to what extent their results still are in the range of the new findings from the CMIP6 Ensemble. A fourth ensemble, consisting of the CMIP6 models, which already offer forcing data for regional dynamical downscaling, is also included. The choice of the CMIP5 GCMs for downscaling EURO-CORDEX RCMs was initially mainly driven by the availability of boundary data. In C3S_34b_Lot2, the matrix of GCM-RCM combinations existing already at the onset of the project has been complemented in a way to enable studies of natural variability, fill as large sub-matrix as possible for the RCP8.5 scenario, and to add a significant amount of simulations for the RCP2.6 scenario. To avoid an ensemble of opportunity when downscaling CMIP6 GCMs in the future, a task force formed within the EURO-CORDEX community. Their work is still ongoing, collecting many different evaluation results of CMIP6 GCMs. The choice of the GCM generally has a larger influence on the climate change signal than the choice of the RCM (Christensen and Kjellström, 2020).

On the global scale, the overall model performance was summarized for CMIP5 in the IPCC Fifth Assessment Report (Flato, 2013). Lately, CMIP5 models have been compared to the results of CMIP6 (Bock et al., 2020). The future global precipitation and temperature results from CMIP6 are compared to CMIP5 by Tebaldi et al. (2021). In this study we will focus on Europe. Previous work of Coppola et al. (2021) and Vautard et al. (2021) on validation and climate change response of the EURO-CORDEX ensemble, their driving GCMs from CMIP5 and a subset of CMIP6 simulations will be complemented with this study by putting the forcing GCMs from CMIP5 into relation to the whole CMIP5 ensemble as well as the results of the CMIP6 ensemble. The size of the CMIP6 ensemble has increased since then, so an updated assessment that we are doing here is also useful in this respect. Comparison of the GCM ensembles with the EURO-CORDEX RCM ensemble is not done here but has been partly covered in other parts of the project (e.g. Vautard et al., 2021; Coppola et al., 2021) and is a field of continued investigation.

1. Model performance from CMIP5 and CMIP6

The goal of this study is to put forcing GCMs used in EURO-CORDEX in the perspective of the whole CMIP5 (Taylor et al., 2012) ensemble and the new CMIP6 (Eyring et al., 2016) ensemble.

Improvements or changes in model performance from CMIP5 to CMIP6 are typically a combination of different factors such as increasing spatial and vertical resolution, a more complete and also an improved and more detailed representation of individual components of the climate system. It is also related to the inclusion of additional Earth system processes that were added in recent years as increasing computing power became available (Bock et al., 2020). Input data, including prescribed emissions and forcing conditions, were continuously refined and further developed. The CMIP6 experiment design for the Scenario Model Intercomparison Project was described in Neill et al. (2018). The experiments produce projections for a set of eight new 21st century scenarios based on the Shared Socio-economic Pathways (SSPs) (Riahi et al., 2017). Some were chosen specifically to provide continuity with the RCPs: SSP1-2.6, SSP2-4.5, SSP4-6.0 and SSP5-8.5, where 2.6 to 8.5 stands for the stratospheric adjusted radiative forcing W/m² by the end of the 21st century. However, it is noted that despite the same nominal forcing levels at the end of the 21st century the forcing scenarios differ. This is a consequence of CMIP5 and CMIP6 concentration pathways differ with respect to their composition across gases (Tebaldi et al., 2020). SSPs aerosol concentration pathways have been improved (Riahi et al., 2017). Figure Appendix A1.1. taken from Tebaldi et al., 2020, shows a comparison of CO_2, CH_4 and N_2O concentrations and radiative forcing conditions for the concentration-driven CMIP5 runs with RCP2.6, RCP4.5, RC8.5 scenarios (Meinshausen et al., 2011) and CMIP6 runs with SSP1-2.6, SSP2-4.5, SSP5-8.5 scenarios (Meinshausen et al., 2020).

1.1 Equilibrium Climate Sensitivity

It has been shown that CMIP6 models depict a higher equilibrium climate sensitivity (ECS) on average than CMIP5 models (Meehl et al., 2020; Zelinka et al., 2020), see Figure 1. One explanation for higher ECS on average in CMIP6 is strengthened cloud feedbacks (Zelinka et al., 2020). ECS provides a single number, defined as the change in global mean surface air temperature resulting from doubling of atmospheric CO_2 concentration compared to preindustrial conditions, once the climate has reached a new equilibrium (Gregory et al., 2004). One explanation for higher ECS on average in CMIP6 is strengthened cloud feedbacks (Zelinka et al., 2020). Bock et al. 2020 calculated the ECS for each GCM, their results for CMIP5 range from 2.1 to 4.7 K and for CMIP6 from 1.8 to 5.6 K. The ECS is important as a higher ECS generally leads to higher climate change signals globally and in most of the regions. The red arrows show which CMIP5 GCMs that have been downscaled in EURO-CORDEX. It is clear that the sample includes models both in the high and mid-range of the ECS span but also that the lowermost 25% of the full span of GCMs, with an ECS below 2.6, are not represented. This indicates that climate sensitivity in the underlying ensemble may be biased high. Any potential impacts on the

European climate cannot be directly inferred and would require more in-depth studies.

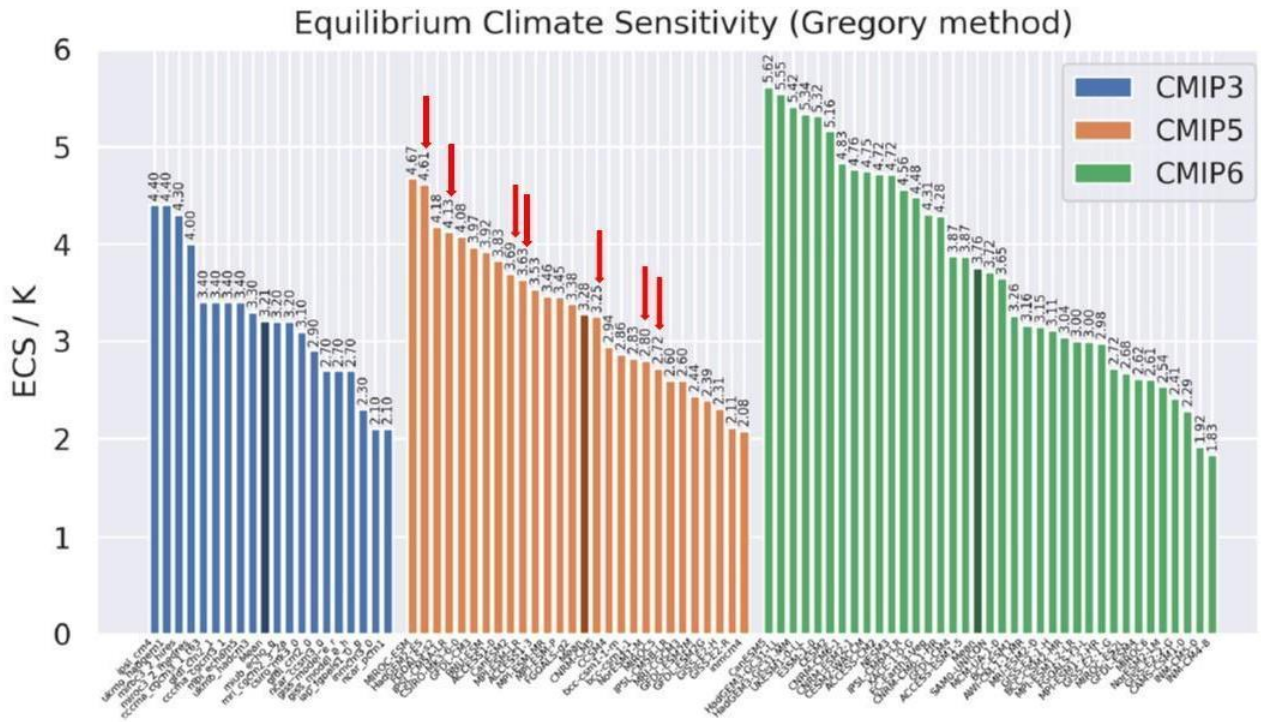

Figure 1. Effective climate sensitivity (ECS) calculated for CMIP3 (blue), CMIP5 (orange), and CMIP6 (green) models using the method from Gregory (Gregory et al., 2004). The ensemble means are indicated by a darker shading of the corresponding bars. The red arrows point to GCMs used as forcing within EURO-CORDEX (ECS of EC-EARTH was not available). Source: (Bock et al., 2020).

2. Evaluation of the historical time period

Globally, the CMIP6 results show a similar or even slightly higher skill in reproducing observed large scale mean surface temperature and precipitation patterns than in CMIP5. The correlation patterns of some important fields such as top of atmosphere (TOA) radiative fluxes, temperature, precipitation and sea level pressure show overall improvements with reduced inter-model spread and higher average skill of the CMIP6 ensemble (Bock et al., 2020).

In the multi-model mean, the magnitudes of the energy balance components are often in agreement with the reference estimates compared to earlier model generations on a global mean basis. The inter-model spread in the representation of main components remains substantial (Wild, 2020.)

McSweeney et al. (2014) analysed the full CMIP5 ensemble to assess their overall performance and advise on the 'best' GCMs to select for regional downscaling. If we only consider CMIP5 GCMs selected for EURO-CORDEX, most GCMs stand within the CMIP5 ensemble performance. However, IPSL-CM5A-LR and IPSL-CM5A-MR show weaknesses (particularly in terms of circulation and

representation of precipitation and temperature annual cycle), CanESM2 and NorESM1-M have circulation biases, while MIROC5 is rated as being implausible in terms of circulation (no clear westerly flow). These findings are in line to later studies analysing both CMIP5 and CMIP6 ensembles.

Brands (2021) analysed the CMIP5 and CMIP6 GCMs ability to represent the regional climate circulation based on 27 cyclonic, anticyclonic and directional (north, northeast, east, southeast, south, southwest, west, northwest) atmospheric circulation patterns in the Northern Hemisphere mid-latitudes as originally defined by Lamb (1972). The patterns are computed using 6-hourly sea-level pressure for the period 1979-2005, and the performances are identified using the mean absolute error of the weather types frequency of the models with regards to reanalyses (ERA-Interim and JRA-55). The models are also grouped depending on their shared components to identify and explain common error structures. In general, all models tend to perform better over the ocean than over the land, and perform poorest over high mountains. Brands (2021) also finds that CMIP6 models tend to perform better than CMIP5, which is mostly attributed to their higher horizontal resolution. The largest improvements are found for model families that performed poorly in CMIP5 (e.g., NorESM2-LM and NorESM2-MM improve upon NorESM1-M, MIROC6 improves upon MIROC5, IPSL-CM6A-LR improves upon IPSL-CM5A-LR and IPSL-CM5A-MR, MPI-ESM1.2-HR with its high-resolution improves upon MPI-ESM-LR and MPI-ESM-MR). The only model that shows a clear performance loss from CMIP5 to CMIP6 is CNRM-CM6-1-HR, despite improved parameterization schemes and higher resolutions in both the atmosphere and the ocean. Among CMIP5 and CMIP6, the EC-EARTH model family generally performs best. Among CMIP6, the better models generally are the simpler atmosphere-ocean coupled GCMs (such as EC-EARTH), therefore less complex than the Earth System Models (ESMs). Among ESMs, NorESM2-MM is generally best, but the Hadley Centre and ACCESS models also perform very well, while MIROC-ESM, IPSL-CM5A-LR and IPSL-CM5A-MR performances are weaker. Models that share the same atmospheric component tend to have similar performance in regional circulation patterns, while GCMs that do not share the same atmospheric component but share the ocean or the land surface component generally have different performance. Internal model variability is shown to only have a small impact on model performance. These results imply that GCM selection should not only be based on model performance criteria but also on model complexity.

The findings of Brands (2021) are consistent with Fernandez-Granja et al., 2021, who also used the weather type classification from Lamb (1972) but based on daily mean sea level pressure and focusing on CMIP5 and CMIP6 GCMs sharing the same model family compared to ERA-Interim, JRA-55, NCEP and ERA-20C reanalyses. The performance of the models is quantified using several metrics based on the weather types frequency, persistence and transition probability from one to another. Using such metrics, Fernandez-Granja et al. (2021) also find an overall improvement from CMIP5 to CMIP6. CMIP5 GCMs that perform well also perform well in the CMIP6 generation. Large improvements are also found from IPSL-CM5A-LR to IPSL-CM6A-LR and from GFDL-ESM2M to GFDL-ESM4, which is also attributed to their higher resolution. Important biases remain, however, in NorESM2-LM and CanESM5 that struggle to accurately simulate transitions from one weather type to another, mostly due to their low horizontal resolution of more than 2 degrees. Cannon (2020) also found an overall improvement in CMIP6 over CMIP5 models using different objective classification methods.

Fabiano et al. (2021) also evaluated CMIP5 and CMIP6 performance during the historical period in representing wintertime mid-latitude weather regimes. The weather regimes are identified using an

Empirical Orthogonal Function decomposition on observed anomalies of daily mean geopotential height at 500 hPa and retaining the four leading modes. For the Euro-Atlantic sector, the 4 regimes identified are the positive and negative phases of the North Atlantic Oscillation (NAO+ and NAO-), the Scandinavian blocking and the Atlantic Ridge. The performance is evaluated in terms of regime centroids, regime frequency bias and variance ratio. They found a general improvement going from CMIP5 to CMIP6 in the Euro-Atlantic sector (performance of individual models is not available).

This short literature review indicates that there is a relatively good performance of the GCMs in representing the large-scale atmospheric circulation in both seasonal means and shorter-term daily variability. It also reveals that the representation is generally better for more high-resolution GCMs than for low-resolution ones and for CMIP6 GCMs over CMIP5 GCMs. We also note here that the RCMs tend to realistically represent the large-scale circulation characteristics as inherited from the GCMs (shown in the deliverable report D2.4.3.4 "Synthesis of EURO-CORDEX simulations as of May 2021" of this project). In the following, we expand the analysis to investigate the performance of the CMIP5 and CMIP6 model ensemble for the European region in reproducing seasonal mean near-surface temperature and precipitation. For the historical time period 1981-2010 the annual and seasonal means are compared to ERA5 averaged over all land points of three SREX regions (Appendix Figure A1.2): Northern Europe (NEU), Western & Central Europe (WCE) and the Mediterranean (MED). For CMIP5 the historical time period that ends in 2005 is extended to 2010 by adding results from the RCP8.5 scenario as this is the scenario for which most runs are available. The difference between the different scenarios RCP8.5, RCP4.5 and RCP2.6 are very small in the five-year period 2006-2010. A direct comparison of the single models of CMIP5 and CMIP6 is difficult, since participating models have changed. We will concentrate on the performance of the different ensembles. In addition, the Appendix contains figures showing the bias for each individual model (Figures A2.1 and A2.2).

2.1 Temperature

The mean temperature and precipitation biases of the GCM ensemble used as boundary forcing for regional climate models within EURO-CORDEX (CMIP5-CORDEX) will be compared to the full CMIP5 GCM ensemble to show how representative the findings are for the historical time period. To investigate how the biases changed in CMIP6 two additional ensembles of GCMs are analysed: the whole CMIP6 GCM ensemble and the CMIP6 GCM ensemble offering boundary data for dynamical downscaling (CMIP6-LBC).

The spread of the annual mean temperature bias is smaller for the CMIP6 than for the CMIP5 ensemble in Northern Europe (NEU) and Western & Central Europe (WCE), but larger in the Mediterranean (MED). The largest bias range is seen for all ensembles in NEU where each median shows a negative bias (Figure 2). The temperature bias spread of the CMIP5 ensemble is larger than the spread of the CMIP5-CORDEX (ensemble downscaled by EURO-CORDEX), but the interquartile range (from 25th to 75th quantile) is similar, except in NEU where it is smaller for all seasons. For single models in the CMIP6 ensemble, a strong cold temperature bias still persists in winter in NEU and some show a very strong warm temperature bias in summer in MED (see Appendix Figure A2.1).

2.2 Precipitation

The spread of the annual bias has reduced in the CMIP6 ensemble compared to CMIP5 in Northern Europe (NEU) and the Mediterranean (MED). Almost all CMIP5 and all CMIP6 GCMs show a median dry bias in the Mediterranean. The spread and interquartile range of CMIP5-CORDEX is smaller than in CMIP5 (Figure 3). The dry bias in summer (JJA) in NEU and Western & Central Europe (WCE) is obvious in most models in CMIP5 and still exists in CMIP6 and even more pronounced in WCE (see Appendix Figure A2.2).

Contrastingly to the dry biases, the CNRM model shows a wet bias in both CMIP5 and CMIP6 in the Mediterranean (Appendix Figure A2.2). These results are consistent with the studies done on global scale for that model (Séférian et al., 2019; Voldoire et al., 2019). The ranges of precipitation and temperature biases for the different regions in Europe (NEU, WCE and MED) are listed in Table 1 for CMIP5 and CMIP6.

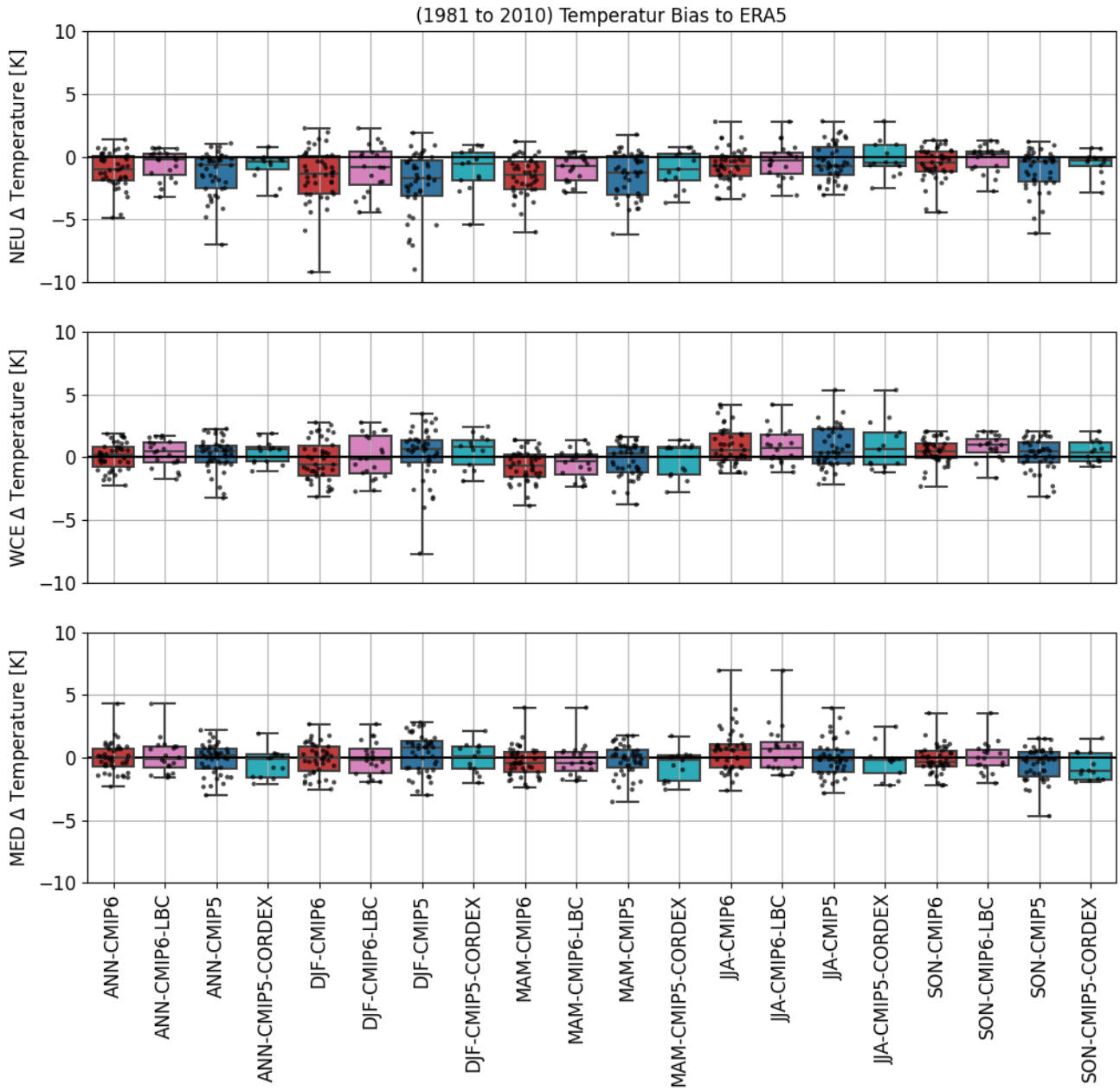

Figure 2. 30-year annual and seasonal mean temperature bias (1981-2010) of CMIP5 and CMIP6 GCMs compared to ERA5 averaged over three European regions, from top to bottom: Northern Europe (NEU), Western & Central Europe (WCE) and Mediterranean (MED). Colored boxes represent the ensemble spread between the 25th and 75th quantile for each ensemble: CMIP6 (red), CMIP6-LBC (provide boundary data for possible future dynamical downscaling) (pink), CMIP5 (blue) and CMIP5-CORDEX (used as forcing within EURO-CORDEX) (cyan). The black bars present the ensemble minimum, median and maximum. The back dots represent the result of each single model of the ensemble. In NEU, DJF-CMIP5 one model is outside of the plotted range with a cold bias of 13.9 K.

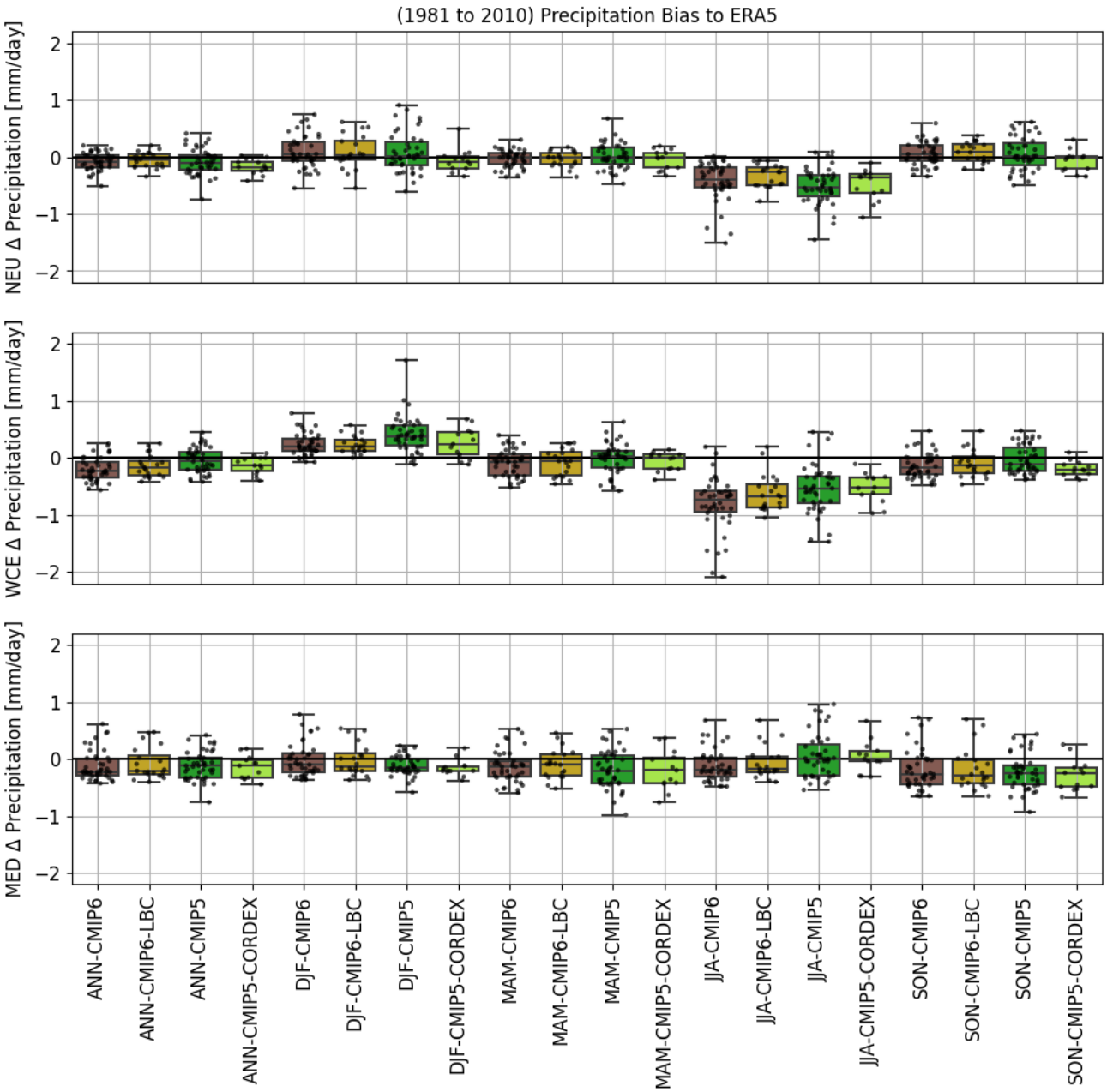

Figure 3. As Fig. 2 but for precipitation and with different colors where CMIP6 (dark brown), CMIP6-LBC (yellow), CMIP5 (dark green) and CMIP5-CORDEX (light green)

Table 1. Ensemble mean and range of CMIP5, CMIP5-CORDEX, CMIP6 and CMIP6-LBC annual temperature and precipitation bias compared to ERA5. The bias values are area means for Northern Europe (NEU), Western & Central Europe (WCE) and the Mediterranean (MED).

Annual mean bias w.r.t. ERA5 (1981-2010)		Temperature [K]	Precipitation [mm/day]
NEU Mean	CMIP5	-0.7	-0.1
	CMIP5-CORDEX	-0.4	-0.2
	CMIP6	-1.1	-0.1
	CMIP6-LBC	-0.3	-0.04
Min. – Max.	CMIP5	-7.1 to 1.1	-0.7 to 0.4
	CMIP5-CORDEX	-3.1 to 0.8	-0.4 to 0.02
	CMIP6	-4.9 to 1.3	-0.5 to 0.2
	CMIP6-LBC	-3.2 to 0.7	-0.3 to 0.2
WCE Mean	CMIP5	0.5	-0.1
	CMIP5-CORDEX	0.6	-0.1
	CMIP6	0.2	-0.2
	CMIP6-LBC	0.4	-0.2
Min. – Max.	CMIP5	-3.3 to 2.3	-0.4 to 0.4
	CMIP5-CORDEX	-1.1 to 1.9	-0.4 to 0.1
	CMIP6	-2.3 to 2.0	-0.6 to 0.3
	CMIP6-LBC	-1.8 to 1.7	-0.4 to 0.3
MED Mean	CMIP5	0.2	-0.1
	CMIP5-CORDEX	-0.1	-0.1
	CMIP6	-0.1	-0.2
	CMIP6-LBC	-0.2	-0.2
Min. – Max.	CMIP5	-3.0 to 2.2	-0.8 to 0.4
	CMIP5-CORDEX	-2.1 to 1.9	-0.4 to 0.2
	CMIP6	-2.3 to 4.6	-0.4 to 0.6
	CMIP6-LBC	-1.6 to 4.3	-0.4 to 0.5

3. Climate Change

On the global scale first results show that the long term-warming range of CMIP5 was exceeded by several models of CMIP6. Tokarska et al. (2020) show that some CMIP6 models with high climate sensitivity project a stronger warming than CMIP5, which is correlated with a stronger warming trend during past decades. Their results highlight that CMIP6 median and spread of future warming may not be representative of a distribution constrained by recent observed trends, although some of the CMIP6 models simulate some individual climate processes more realistically than CMIP5. CMIP6 models that have a climate sensitivity in the range of CMIP5 models show warming trends that are consistent with observations. This points to the fact that careful evaluation of models is needed before using them for climate change assessment depending on application.

Also, the change in the forcing datasets from CMIP5 to CMIP6 could substantially lead to the larger warming at the end of the century (Wyser et al., 2020): A study with the EC-Earth model finds that about half of the difference in warming by the end of the century when comparing CMIP5 RCPs and their updated CMIP6 counterparts is due to differences in effective radiative forcing conditions at 2100 of up to 1 W/m². Preliminary results with the Canadian model CanESM2 confirm the significant role of higher radiative forcing conditions found with EC-Earth (Tebaldi et al., 2020). We note here that such differences can occur in complex GCMs despite the fact that the nominal forcing appears to be very similar in the experiments as discussed in Figure A1.1.

Several studies are already performed to tackle the wide ensemble spread and strong warming signal in the CMIP6 ensemble e.g. by weighting the models by performance and independence (Brunner et al., 2020) or partitioning uncertainty in projections of future climate change into contributions from internal variability, model response uncertainty and emission scenarios (Lehner et al., 2020).

In the Euro-Atlantic during winter the CMIP6 models project a positive trend in frequency and persistence of the NAO+, particularly in the SSP5-8.5 scenario, which is larger than in the CMIP5 RCP8.5 projections (Fabiano et al., 2021). Concurrently, CMIP6 projects a decrease in the frequency of the Scandinavian blocking and Atlantic Ridge regimes, with a trend under SSP5-8.5 that is similar to CMIP5 RCP8.5. These projections are explained by a zonalisation of the mid-latitude circulation and a squeezing of the eddy-driven jet distribution around its central position (Oudar et al., 2020a). As the jet is more often in its central position and less in a tilted position, the frequency of NAO+ increases while it decreases for the Scandinavian blocking and Atlantic Ridge. This decrease implies a decrease in blocking frequency over Europe projected by both CMIP5 and CMIP6 ensembles (Davini and D'Andrea, 2020). A consequence of such a decrease in frequency and/or persistence of blockings is that cold winter conditions get less common in favor of more mild weather dominated situations. The stronger increase in the frequency of NAO+ in CMIP6 compared to CMIP5 agrees with the intensification of the North Atlantic storm track activity (Harvey et al., 2020). The storm track is therefore less tilted towards high latitudes, which is in line with the decrease in frequency of the Atlantic Ridge, which tends to push the jet poleward. Fabiano et al. (2021) therefore find that CMIP6 projects an amplified increase in winter precipitation over Northern Europe, with a higher risk of flooding, and an amplified decrease in Southern Europe, with a higher risk of droughts. The authors

also found that model spreads in CMIP5 RCP8.5 and CMIP6 SSP5-8.5 projections are mostly driven by the polar stratospheric temperature (a warmer polar stratosphere leads to a decrease in NAO+ and an increase in NAO- due to a weaker polar vortex) and the Arctic Amplification (leading to a weakening and an equatorward shift of the jet). These results are consistent with Oudar et al. (2020b); Zappa and Shepherd (2017).

The climate change response of the EURO-CORDEX ensemble, their driving GCMs from CMIP5 and a set of CMIP6 simulations have been analyzed for RCP2.6, SSP1-2.6 and RCP8.5, SSP5-8.5 (Coppola et al., 2020). In Northern Europe, they found a maximum warming and precipitation increase in all ensembles in winter and in summer. In the Mediterranean, maximum warming occurs along with a precipitation decrease. Here, the analysis of GCM ensembles by Coppola et al. (2020) will be complemented with analysis of the whole CMIP5 ensemble and an enlarged CMIP6 ensemble. Their study was restricted to the CMIP5 GCMs used as forcing in EURO-CORDEX and a small set of CMIP6 GCMs available at the time of their study. The analysis here is restricted to the GCMs and we do not assess the RCM EURO-CORDEX ensemble.

The mean temperature and precipitation change of the GCM ensemble used as boundary forcing for regional climate models within EURO-CORDEX (CMIP5-CORDEX) will be compared to the full CMIP5 GCM ensemble to show how representative the findings are on predicted temperature and precipitation change. To investigate how valid these results will be in the future two additional more recent ensembles of GCMs are analysed: the whole CMIP6 GCM ensemble and the CMIP6 GCM ensemble offering boundary data for dynamical downscaling (CMIP6-LBC).

The 30-year mean annual and seasonal temperature and precipitation change compared to the historical period 1981-2010 is calculated for two time slices 2036-2065 and 2070-2099. For each region NEU, WCE, MED we will compare the CMIP5 results for scenario RCP2.6, RCP4.5, RCP8.5 with their corresponding scenarios of CMIP6 SSP1-2.6, SSP2-4.5, SSP5-8.5. Since the EURO-CORDEX community plans to downscale SSP3-7.0, for which there is no corresponding RCP-scenario in CMIP5, it is additionally added to the figures.

Due to the large number of figures, we will concentrate here on the annual mean change in 2070-2099 and all further figures on seasonal change and annual cycle are in the Appendix (sections 3-8). In the Appendix (section 9) there are also tables containing the CMIP5 and CMIP6 models used in this study (Tables A9.1-A9.2) and in the literature referenced in this report (Tables A9.3-A9.4).

3.1 Mean temperature change

At the end of the 21st century (2070-2099), the median and interquartile spread of the annual temperature increase is more pronounced in all scenarios of CMIP6 compared to their corresponding scenarios of CMIP5 (Figure 4). CMIP5-CORDEX only covers half of the range of the CMIP5 ensemble and less in NEU. The CMIP5-CORDEX ensemble does not cover the upper quarter of the CMIP6 ensemble. The annual mean temperature of the CMIP5-CORDEX and CMIP5 ensemble are very similar. In Northern Europe (NEU) the GCM FIO-ESM depicts a temperature decrease, which enlarges the ensemble spread from minimum to maximum of the CMIP5, but the interquartile spread of CMIP5

is still less compared to CMIP6. Generally, the range of the annual temperature change decreases from North to South and increases with time. Northern Europe shows a stronger warming in winter (Appendix, Figs. A3.1-A3.4). This stronger warming is caused by snow albedo feedback due to the reduction of continental snow cover over large areas. The structure of the mean annual cycle of the temperature change does not change from CMIP5 to CMIP6. NEU shows the strongest warming in winter, WCE and MED the strongest warming in summer (Appendix, Figs. A6.1-A6.6). The mean annual cycle of the CMIP5 ensemble does not differ to the mean of the CMIP5-CORDEX ensemble. Individual models show a strong warming for RCP8.5/SSP5-8.5 (Appendix, Figs. A6.1-A6.6). For all regions and scenarios, the smallest temperature change is depicted in spring (MAM).

The maximum temperature increase in CMIP6 is higher than in CMIP5 (Fig. 4). This could be explained by higher radiative forcing and higher climate sensitivities in a subset of the CMIP6 models. One example is the strong temperature increase projected by individual CMIP6 models in summer in WCE (Appendix Fig. A3.3 and Fig. A6.2): CanESM5 (ECS: 5.62), HadGEM3-GC31-LL (ECS:5.55), HadGEM3-GC31-MM (ECS: 5.42), IPSL-CM6A-LR (ECS: 4.56), UKESM1-0-LL (ECS: 5.43). All these models have a high equilibrium climate sensitivity, which is in most cases above the maximum ECS of CMIP5 (4.67) and could be partly an explanation. In addition, these individual models show a precipitation decrease (Appendix Fig. A7.4). To be sure what caused this large temperature increase in WCE in summer a detailed analysis of the atmospheric circulation and a process-based analysis would be needed.

3.2 Mean precipitation change

The mean annual precipitation increases (2070-2099) for all scenarios in Northern Europe (NEU) and decreases in the Mediterranean (MED) (Figure 5). CMIP5-CORDEX only covers around half of the full spread of the CMIP5 ensemble and it is even less in NEU, as models with high precipitation increase are not included. In WCE and MED models with strong precipitation decrease are not included in the CMIP5-CORDEX ensemble. The median of the CMIP5-CORDEX ensemble corresponds quite well with the CMIP5 ensemble. In NEU the ensemble range of the annual precipitation change in CMIP5 is larger than the range in CMIP6 for all scenarios and very similar in WCE and MED. In NEU and WCE the median of the precipitation change is slightly higher in CMIP6 than in CMIP5 during winter and lower during summer (Appendix, Figs. A4.1 and A4.3). The mean annual cycle of the precipitation change, with increasing precipitation in winter and decreasing precipitation in summer, is more pronounced in CMIP6 compared to CMIP5 comparing the corresponding scenarios in these regions (Appendix, Figs. A7.1-A7.6). In MED the precipitation decreases for every season through the year in both CMIP5 and CMIP6. These structures intensify with increasing emission scenarios for all scenarios. For the annual cycle, no distinct difference is found comparing the ensemble mean of CMIP5 with CMIP5-CORDEX. An additional seasonal feature occurs in WCE, where the ensemble spread decreases in summer and increases in winter from CMIP5 to CMIP6. The amplification of winter precipitation changes in NEU and WCE and drying in MED is consistent with the findings from Fabiano et al., 2021. The CMIP5-CORDEX ensemble is spanning the center space of temperature and precipitation change of the CMIP5 and CMIP6 ensemble, but in winter it misses the upper range of temperature change in WCE and NEU (Appendix, Fig. A5.1).

Additional information for temperature and precipitation change for each individual model is provided in the Appendix (Figs. A6.1-A6.6 and A7.1-A7.6).

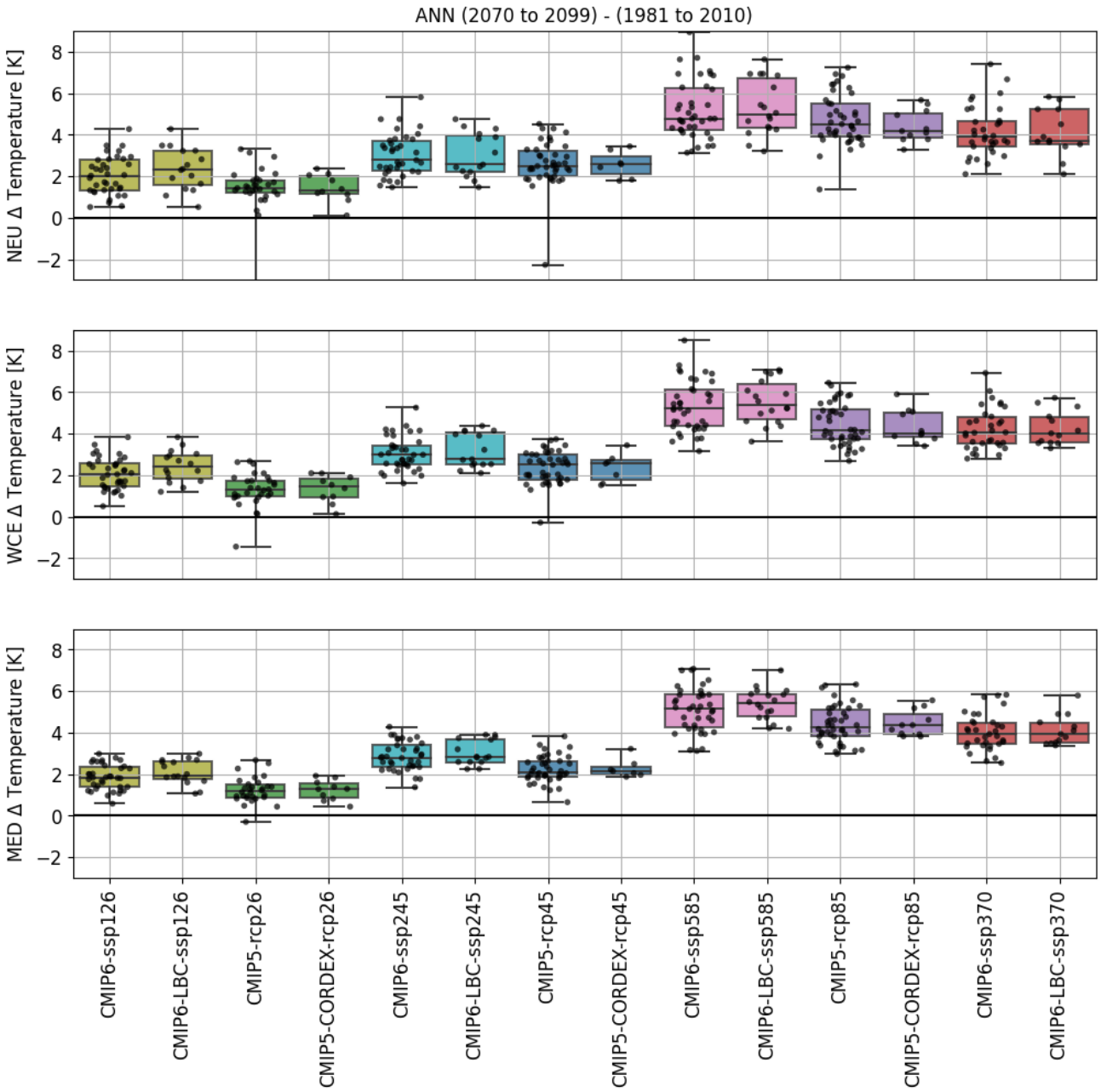

Figure 4. 30-year annual mean temperature change (2070-2099) - (1981-2010) for scenario SSP1-2.6, SSP2-4.5, SSP5-8.5, SSP3-7.0 (lighter colors: lime, cyan, pink, red) and scenario RCP2.6, RCP4.5, RCP8.5 (darker colors: green, blue, purple) averaged over three European regions, from top to bottom: Northern Europe (NEU), Western & Central Europe (WCE) and the Mediterranean (MED). Colored boxes represent the ensemble spread between the 25th and 75th quantile for each ensemble: CMIP6, CMIP6-LBC (provide boundary data for dynamical downscaling), CMIP5 and CMIP5-CORDEX (used as forcing within EURO-CORDEX). The black bars represent the ensemble minimum, median and maximum. The black dots represent the result of each single model of the ensemble. In NEU, CMIP5-RCP2.6 one model is outside the shown range with a temperature decrease of -5,1 K.

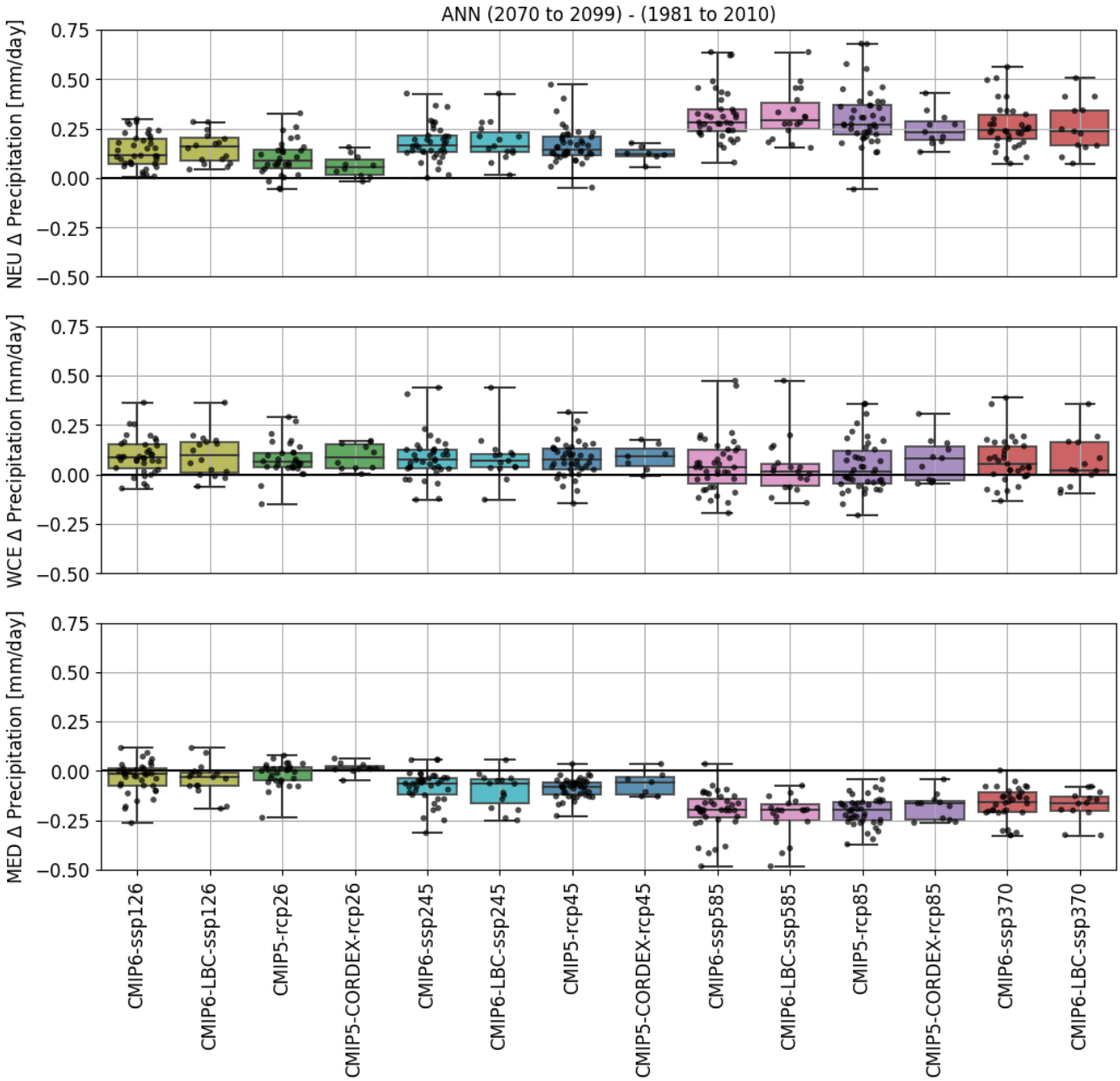

Figure 5. 30-year annual mean precipitation change (2070-2099) - (1981-2010) for scenario SSP1-2.6, SSP2-4.5, SSP5-8.5, SSP3-7.0 (lighter colors: lime, cyan, pink, red) and scenario RCP2.6, RCP4.5, RCP8.5 (darker colors: green, blue, purple) averaged over three European regions, from top to bottom: Northern Europe (NEU), Western & Central Europe (WCE) and Mediterranean (MED). Colored boxes present the ensemble spread between the 25th and 75th quantile for each ensemble: CMIP6, CMIP6-LBC (provide boundary data for dynamical downscaling), CMIP5 and CMIP5-CORDEX (used as forcing within EURO-CORDEX). The black bars present the ensemble minimum, median and maximum. The back dots represent the result of each single model of the ensemble.

4. Summary

Globally, an improvement with respect to observations of the CMIP6 ensemble results compared to the precursor CMIP5 ensemble was confirmed by many authors. They also confirmed improvement of the ability of GCMs to represent the regional climate circulation in northern latitudes. All still find a remaining substantial inter-model spread in the representation. Each CMIP5/CMIP6 ensemble consists of one member per GCM, internal variability was not investigated so far (exception: we added 2 members of MPI-ESM-LR and 1 member of EC-EARTH to CMIP5, because these particular members got downscaled by EURO-CORDEX).

This study confirms the previous findings for CMIP5 and downscaled CMIP5 results for Europe (e.g. Coppola et al. (2021)) for temperature and precipitation change at the end of the 21st century. Regional and seasonal features of temperature and precipitation changes in Europe exist in the results of the CMIP5 and CMIP6 ensemble, which are a distinct precipitation and temperature increase during winter in Northern Europe and pronounced drying in the Mediterranean during summer in RCP8.5/SSP5-8.5. The median of the temperature change of each scenario from CMIP6 is higher than its corresponding scenario in CMIP5. In Northern and Western & Central Europe, the median of the precipitation change is slightly higher in CMIP6 than in CMIP5 during winter and lower during summer. Major changes are found in Western & Central Europe during summer showing a distinct drying and an enlarged range of temperature change for SSP5-8.5.
The CMIP5 models used as forcing for EURO-CORDEX RCMs cover half of the full spread of the temperature and precipitation change of the CMIP5 ensemble, but less in NEU. The median of the annual precipitation and temperature change of the CMIP5-CORDEX ensemble is similar to the median of the CMIP5 ensemble.

Generally former findings are confirmed by the CMIP6 ensemble, but some of the CMIP6 models show a drying and stronger temperature increase in summer (NEU, WCE) and very high precipitation increase in WCE in winter, which has not been projected before. Further process-based analysis is necessary to understand these extremes. Furthermore, an analysis of the circulation patterns for all available CMIP6 models needs to be completed. In the future we plan to extend these studies by assessing the sea surface temperature and arctic climate as well as extending the literature review on CMIP5/CMIP6. Eventually we plan to combine all information on the historical bias and climate change of the CMIP5 and CMIP6 ensemble (similar to McSweeney et al., 2014) to give the regional climate modelers a fundamental background for their decisions.

It is clear from the analysis shown here that the CMIP5 and CMIP6 ensembles both show a great deal of overlap but also differences. Any user of climate change information needs to carefully consider which dataset that best serves his/her purposes. If regional climate projections from EURO-CORDEX driven by CMIP5 GCMs are used it is crucial to know how these GCMs relate to the wider full range of CMIP5 models and possibly to the CMIP6 ensemble. This report can give some guidance here.

5. Data

5.1 Data processing

CMIP5, CMIP6 data are provided at the ESGF (Earth System Grid Federation, e.g. https://esgf-data.dkrz.de/projects/esgf-dkrz) and at the Copernicus Climate Data Store https://cds.climate.copernicus.eu.

From the CMIP5 and CMIP6 ensemble, we arbitrarily selected the first realization of each model. Only if the first realization was not available for a specific scenario, we selected another realization, so that we would not miss out any climate model (Appendix: Table A9.1 and A9.2).
Some modelling groups did not provide a land see mask to their model results in which case we used the land see mask from CRU-TS4.02.

The models used in the literature on weather types and circulation change are summarized in the Appendix: Table A9.3 and A9.4.

ERA5 monthly averaged data on single levels from 1979 to present, Copernicus Climate Change Service (C3S), (2017). ERA5: Fifth generation of ECMWF atmospheric reanalysis of the global climate, edited, Copernicus Climate Change Service Climate Data Store (CDS). https://cds.climate.copernicus.eu/cdsapp#!/home, DOI: 10.24381/cds.f17050d7

6. References

Bock, L., Lauer, A., Schlund, M., Barreiro, M., Bellouin, N., Jones, C., Meehl, G. A., Predoi, V., Roberts, M. J. and Eyring, V.: Quantifying Progress Across Different CMIP Phases With the ESMValTool, J. Geophys. Res. Atmos., 125(21), 1–28, doi:10.1029/2019JD032321, 2020.

Brands, S.: A circulation-based performance atlas of the CMIP5 and 6 models for regional climate studies in the northern hemisphere, Geosci. Model Dev. Discuss., (February), 1–48, doi:10.5194/gmd-2020-418, 2021.

Brunner, L., Pendergrass, A. G., Lehner, F., Merrifield, A. L., Lorenz, R. and Knutti, R.: Reduced global warming from CMIP6 projections when weighting models by performance and independence, Earth Syst. Dyn., 11(4), 995–1012, doi:10.5194/esd-11-995-2020, 2020.

Cannon, A. J.: Reductions in daily continental-scale atmospheric circulation biases between generations of global climate models: CMIP5 to CMIP6, Environ. Res. Lett., 15(6), doi:10.1088/1748-9326/ab7e4f, 2020.

Christensen, O. B. and Kjellström, E.: Partitioning uncertainty components of mean climate and climate change in a large ensemble of European regional climate model projections, Clim. Dyn., doi:10.1007/s00382-020-05229-y, 2020.

Coppola, E., Nogherotto, R., Ciarlò, J. M., Giorgi, F., Meijgaard, E., Kadygrov, N., Iles, C., Corre, L., Sandstad, M., Somot, S., Nabat, P., Vautard, R., Levavasseur, G., Schwingshackl, C., Sillmann, J., Kjellström, E., Nikulin, G., Aalbers, E., Lenderink, G., Christensen, O. B., Boberg, F., Sørland, S. L., Demory, M., Bülow, K., Teichmann, C., Warrach-Sagi, K. and Wulfmeyer, V.: Assessment of the European climate projections as simulated by the large EURO-CORDEX regional and global climate model ensemble., 2020.

DAVINI, P. and D'ANDREA, F.: From CMIP3 to CMIP6: Northern hemisphere atmospheric blocking simulation in present and future climate, J. Clim., 33(23), 10021–10038, doi:10.1175/JCLI-D-19-0862.1, 2020.

Eyring, V., Bony, S., Meehl, G. A., Senior, C. A., Stevens, B., Stouffer, R. J. and Taylor, K. E.: Overview of the Coupled Model Intercomparison Project Phase 6 (CMIP6) experimental design and organization, Geosci. Model Dev., 9(5), 1937–1958, doi:10.5194/gmd-9-1937-2016, 2016.

Fabiano, F., Meccia, V. L., Davini, P., Ghinassi, P. and Corti, S.: A regime view of future atmospheric circulation changes in northern mid-latitudes, Weather Clim. Dyn., 2(1), 163–180, doi:10.5194/wcd-2-163-2021, 2021.

Fernandez-Granja, J. A., Casanueva, A., Bedia, J. and Fernandez, J.: Improved atmospheric circulation over Europe by the new generation of CMIP6 earth system models, Clim. Dyn., doi:10.1007/s00382-021-05652-9, 2021.

Flato, G., J. Marotzke, B. Abiodun, P. Braconnot, S.C. Chou, W. Collins, P. Cox, F. Driouech, S. Emori, V. Eyring, C. Forest, P. Gleckler, E. Guilyardi, C. Jakob, V. Kattsov, C. Reason and M. Rummukainen, 2013: Evaluation of Climate Models. In: Climate Change 2013: The Physical Science Basis. Contribution of Working Group I to the Fifth Assessment Report of the Intergovernmental Panel on Climate Change [Stocker, T.F., D. Qin, G.-K. Plattner, M. Tignor, S.K. Allen, J. Boschung, A. Nauels, Y. Xia, V. Bex and P.M. Midgley (eds.)]. Cambridge University Press, Cambridge, United Kingdom and New York, NY, USA.

Gregory, J. M., Ingram, W. J., Palmer, M. A., Jones, G. S., Stott, P. A., Thorpe, R. B., Lowe, J. A., Johns, T. C. and Williams, K. D.: A new method for diagnosing radiative forcing and climate sensitivity, Geophys. Res. Lett., 31(3), 2–5, doi:10.1029/2003GL018747, 2004.

Harvey, B. J., Cook, P., Shaffrey, L. C. and Schiemann, R.: The Response of the Northern Hemisphere Storm Tracks and Jet Streams to Climate Change in the CMIP3, CMIP5, and CMIP6 Climate Models, J. Geophys. Res. Atmos., 125(23), 1–10, doi:10.1029/2020JD032701, 2020.

Lehner, F., Deser, C., Maher, N., Marotzke, J., Fischer, E. M., Brunner, L., Knutti, R. and Hawkins, E.: Partitioning climate projection uncertainty with multiple large ensembles and CMIP5/6, Earth Syst. Dyn., 11(2), 491–508, doi:10.5194/esd-11-491-2020, 2020.

McSweeney, C. F., Jones, R. G., Lee, R. W. and Rowell, D. P.: Selecting CMIP5 GCMs for downscaling over multiple regions, Clim. Dyn., 44(11–12), 3237–3260, doi:10.1007/s00382-014-2418-8, 2014.

Meehl, G. A., Senior, C. A., Eyring, V., Flato, G., Lamarque, J.-F. F., Stouffer, R. J., Taylor, K. E. and Schlund, M.: Context for interpreting equilibrium climate sensitivity and transient climate response from the CMIP6 Earth system models, Sci. Adv., 6(26), eaba1981, doi:10.1126/sciadv.aba1981, 2020.

Neill, B. C. O., Tebaldi, C., Vuuren, D. P. Van, Eyring, V., Friedlingstein, P., Hurtt, G., Knutti, R., Kriegler, E., Lamarque, J., Lowe, J., Meehl, G. A. and Moss, R.: The Scenario Model Intercomparison Project (ScenarioMIP) for CMIP6, , 3461–3482, doi:10.5194/gmd-9-3461-2016, 2018.

Oudar, T., Cattiaux, J. and Douville, H.: Drivers of the Northern Extratropical Eddy-Driven Jet Change in CMIP5 and CMIP6 Models, Geophys. Res. Lett., 47(8), 1–9, doi:10.1029/2019GL086695, 2020a.

Oudar, T., Cattiaux, J. and Douville, H.: Drivers of the Northern Extratropical Eddy-Driven Jet Change in CMIP5 and CMIP6 Models, Geophys. Res. Lett., 47(8), 1–9, doi:10.1029/2019GL086695, 2020b.

Riahi, K., van Vuuren, D. P., Kriegler, E., Edmonds, J., O'Neill, B. C., Fujimori, S., Bauer, N., Calvin, K., Dellink, R., Fricko, O., Lutz, W., Popp, A., Cuaresma, J. C., KC, S., Leimbach, M., Jiang, L., Kram, T., Rao, S., Emmerling, J., Ebi, K., Hasegawa, T., Havlik, P., Humpenöder, F., Da Silva, L. A., Smith, S., Stehfest, E., Bosetti, V., Eom, J., Gernaat, D., Masui, T., Rogelj, J., Strefler, J., Drouet, L., Krey, V., Luderer, G., Harmsen, M., Takahashi, K., Baumstark, L., Doelman, J. C., Kainuma, M., Klimont, Z., Marangoni, G., Lotze-Campen, H., Obersteiner, M., Tabeau, A. and Tavoni, M.: The Shared Socioeconomic Pathways and their energy, land use, and greenhouse gas emissions implications: An overview, Glob. Environ. Chang., 42, 153–168, doi:10.1016/j.gloenvcha.2016.05.009, 2017.

Séférian, R., Nabat, P., Michou, M., Saint-Martin, D., Voldoire, A., Colin, J., Decharme, B., Delire, C., Berthet, S., Chevallier, M., Sénési, S., Franchisteguy, L., Vial, J., Mallet, M., Joetzjer, E., Geoffroy, O., Guérémy, J. F., Moine, M. P., Msadek, R., Ribes, A., Rocher, M., Roehrig, R., Salas-y-Mélia, D., Sanchez, E., Terray, L., Valcke, S., Waldman, R., Aumont, O., Bopp, L., Deshayes, J., Éthé, C. and Madec, G.: Evaluation of CNRM Earth System Model, CNRM-ESM2-1: Role of Earth System Processes in Present-Day and Future Climate, J. Adv. Model. Earth Syst., 11(12), 4182–4227, doi:10.1029/2019MS001791, 2019.

Taylor, K. E., Stouffer, R. J. and Meehl, G. A.: An overview of CMIP5 and the experiment design, Bull. Am. Meteorol. Soc., 93(4), 485–498, doi:10.1175/BAMS-D-11-00094.1, 2012.

Tebaldi, C., Debeire, K., Eyring, V., Fischer, E., Fyfe, J., Friedlingstein, P., Knutti, R., Lowe, J., O'Neill, B., Sanderson, B., Van Vuuren, D., Riahi, K., Meinshausen, M., Nicholls, Z., Tokarska, K., Hurtt, G., Kriegler, E., Meehl, G., Moss, R., Bauer, S., Boucher, O., Brovkin, V., Yhb, Y., Dix, M., Gualdi, S., Guo, H., John, J., Kharin, S., Kim, Y. H., Koshiro, T., Ma, L., Olivié, D., Panickal, S., Qiao, F., Rong, X., Rosenbloom, N., Schupfner, M., Séférian, R., Sellar, A., Semmler, T., Shi, X., Song, Z., Steger, C., Stouffer, R., Swart, N.,

Tachiiri, K., Tang, Q., Tatebe, H., Voldoire, A., Volodin, E., Wyser, K., Xin, X., Yang, S., Yu, Y. and Ziehn, T.: Climate model projections from the Scenario Model Intercomparison Project (ScenarioMIP) of CMIP6, Earth Syst. Dyn., 12(1), 253–293, doi:10.5194/esd-12-253-2021, 2021.

Tokarska, K. B., Stolpe, M. B., Sippel, S., Fischer, E. M., Smith, C. J., Lehner, F. and Knutti, R.: Past warming trend constrains future warming in CMIP6 models, Sci. Adv., 6(12), 1–14, doi:10.1126/sciadv.aaz9549, 2020.

Vautard, R., Kadygrov, N., Iles, C., Boberg, F., Buonomo, E., Bülow, K., Coppola, E., Corre, L., Meijgaard, E., Nogherotto, R., Sandstad, M., Schwingshackl, C., Somot, S., Aalbers, E., Christensen, O. B., Ciarlò, J. M., Demory, M., Giorgi, F., Jacob, D., Jones, R. G., Keuler, K., Kjellström, E., Lenderink, G., Levavasseur, G., Nikulin, G., Sillmann, J., Solidoro, C., Sørland, S. L., Steger, C., Teichmann, C., Warrach-Sagi, K. and Wulfmeyer, V.: Evaluation of the large EURO-CORDEX regional climate model ensemble., 2020.

Voldoire, A., Saint-Martin, D., Sénési, S., Decharme, B., Alias, A., Chevallier, M., Colin, J., Guérémy, J. F., Michou, M., Moine, M. P., Nabat, P., Roehrig, R., Salas y Mélia, D., Séférian, R., Valcke, S., Beau, I., Belamari, S., Berthet, S., Cassou, C., Cattiaux, J., Deshayes, J., Douville, H., Ethé, C., Franchistguy, L., Geoffroy, O., Lévy, C., Madec, G., Meurdesoif, Y., Msadek, R., Ribes, A., Sanchez-Gomez, E., Terray, L. and Waldman, R.: Evaluation of CMIP6 DECK Experiments With CNRM-CM6-1, J. Adv. Model. Earth Syst., doi:10.1029/2019MS001683, 2019.

van Vuuren, D. P., Edmonds, J., Kainuma, M., Riahi, K., Thomson, A., Hibbard, K., Hurtt, G. C., Kram, T., Krey, V., Lamarque, J. F., Masui, T., Meinshausen, M., Nakicenovic, N., Smith, S. J. and Rose, S. K.: The representative concentration pathways: An overview, Clim. Change, 109(1), 5–31, doi:10.1007/s10584-011-0148-z, 2011.

Wild, M.: The global energy balance as represented in CMIP6 climate models, Clim. Dyn., 55(3–4), 553–577, doi:10.1007/s00382-020-05282-7, 2020.

Wyser, K., Kjellström, E., Koenigk, T., Martins, H. and Döscher, R.: Warmer climate projections in EC-Earth3-Veg: the role of changes in the greenhouse gas concentrations from CMIP5 to CMIP6, Environ. Res. Lett., 15(5), 054020, doi:10.1088/1748-9326/ab81c2, 2020.

Zappa, G. and Shepherd, T. G.: Storylines of atmospheric circulation change for European regional climate impact assessment, J. Clim., 30(16), 6561–6577, doi:10.1175/JCLI-D-16-0807.1, 2017.

Zelinka, M. D., Myers, T. A., McCoy, D. T., Po-Chedley, S., Caldwell, P. M., Ceppi, P., Klein, S. A. and Taylor, K. E.: Causes of Higher Climate Sensitivity in CMIP6 Models, Geophys. Res. Lett., 47(1), 1–12, doi:10.1029/2019GL085782, 2020.

7. Appendix

Table of Contents, Appendix

1. Concentration pathways and regions

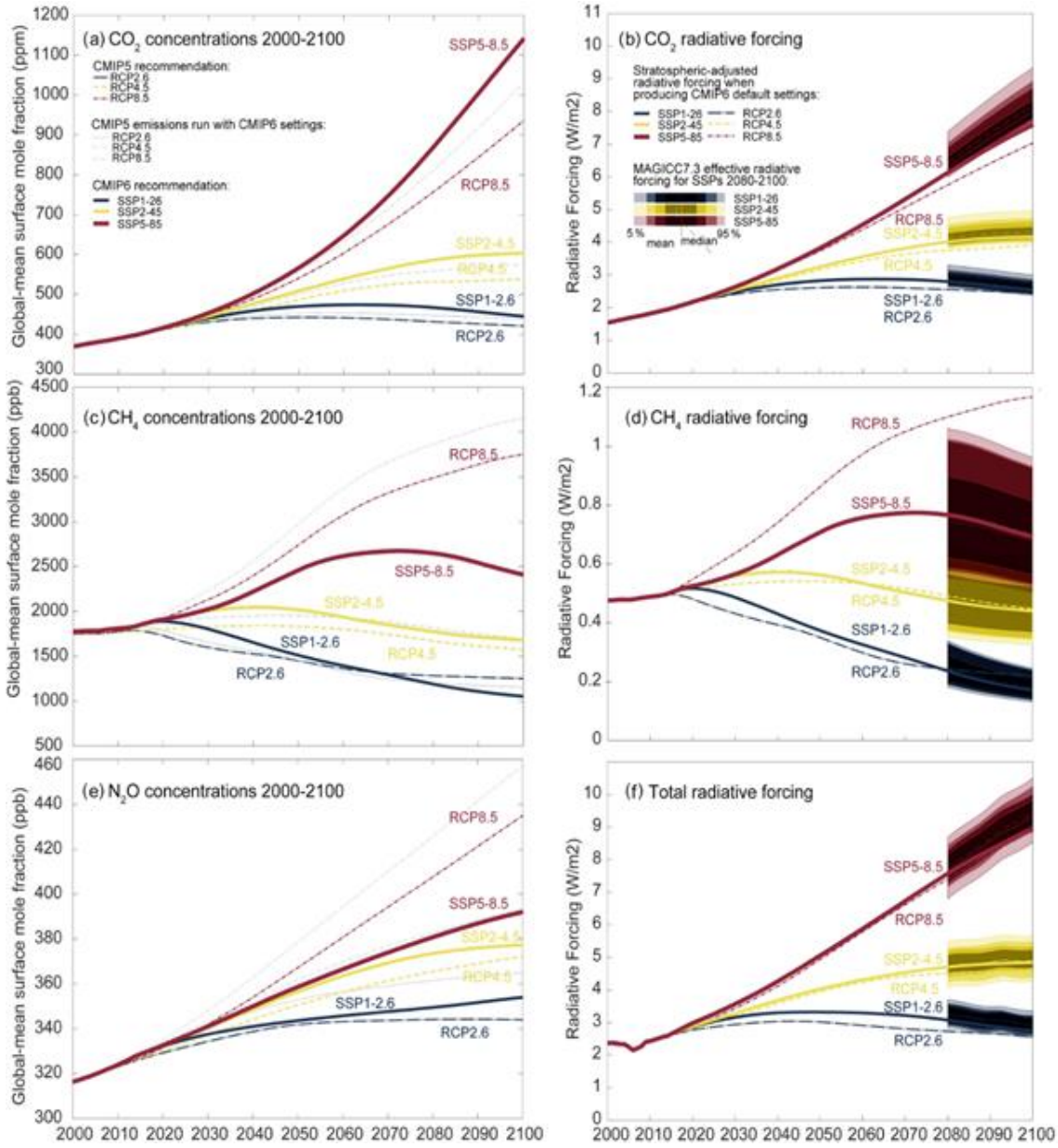

Figure A1.1. (source: Figure 7 of Tebaldi et al., 2020). Comparison of CO_2, CH_4 and N_2O concentrations (left panels) and radiative forcings (right panels) for the concentration-driven CMIP5 runs with RCP2.6, RCP4.5, RCP8.5 scenarios (Meinshausen et al., 2011) and CMIP6 runs with SSP1-2.6, SSP2-4.5, SSP5-8.5 scenarios (Meinshausen et al., 2020). The higher scenario (SSP5-8.5) features higher CO_2 concentrations compared to RCP8.5 (panel a) largely due to updated carbon cycle settings. To illustrate this, CO_2 concentrations calculated using RCP8.5 emissions, but with the same updated carbon cycle settings as in SSP5-8.5, are shown with a thin dashed line in panel a. The methane and nitrous oxide concentrations are lower in SSP5-8.5 than in RCP8.5 (panels c, e). The resulting stratospheric-adjusted radiative forcings (SARFs) match comparing the nameplate radiative forcing levels in 2100 according to the integrated assessment model MAGICC6.8 with IPCC-AR5-consistent settings; see panels (b, d, f).

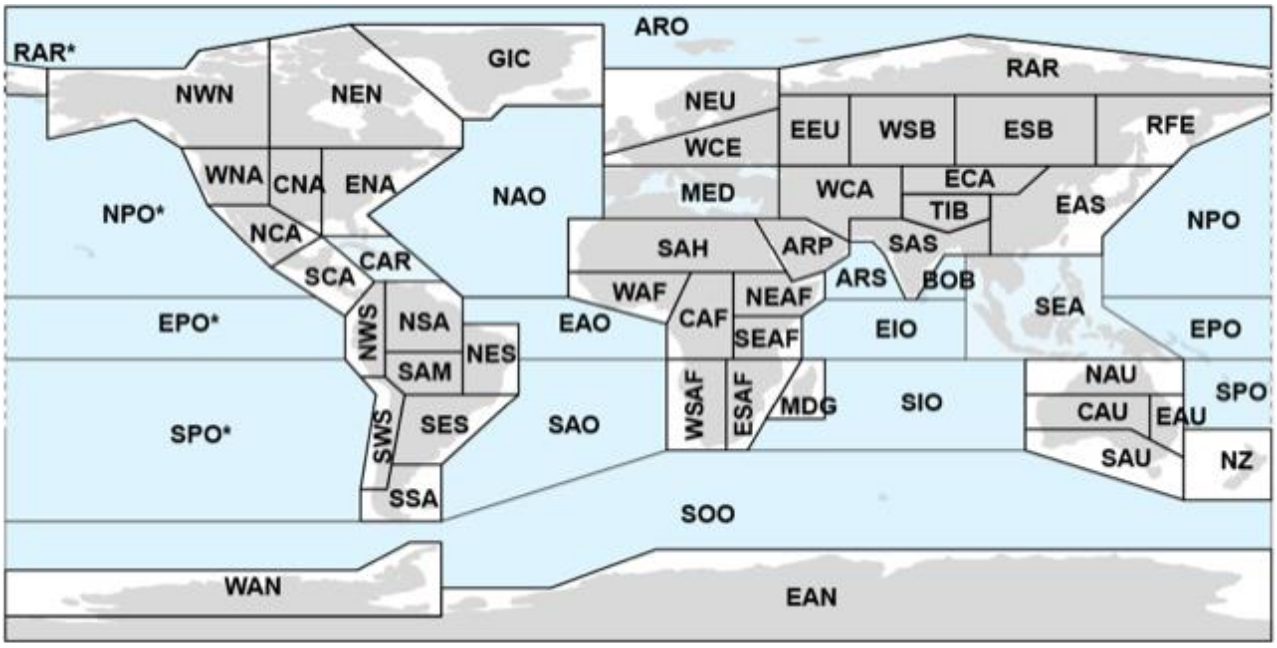

Figure A1.2. Northern Europe (NEU), Western & Central Europe (WCE) and Mediterranean (MED) are the regions, which are analyzed (Iturbide et al., 2020).

2. Evaluation 1981-2010

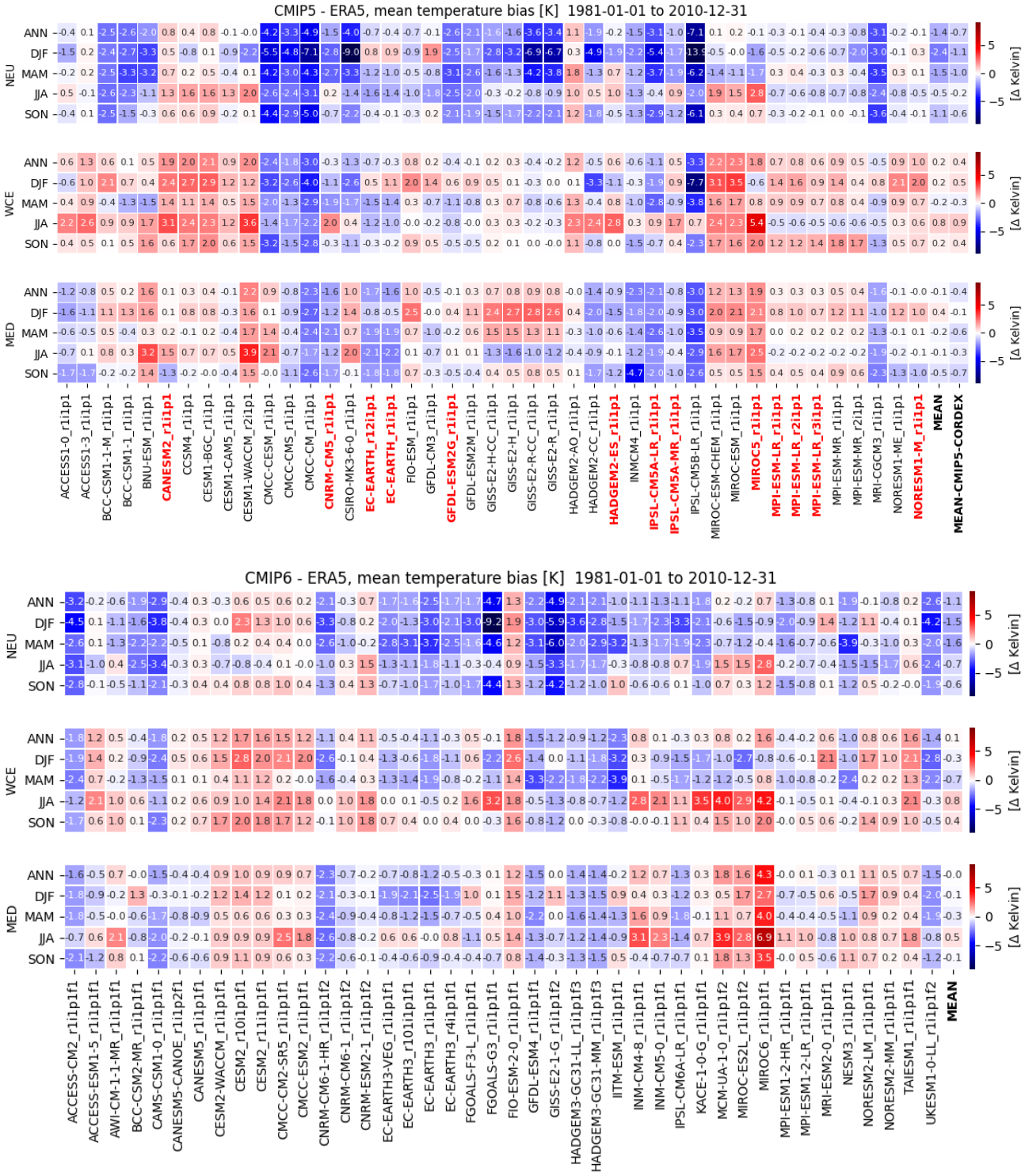

Figure A2.1. 30-year annual mean and seasonal mean temperature bias (1981-2010) of CMIP5 (top), the CMIP5 GCMs used as forcing for the EURO-CORDEX RCMs are highlighted in red and CMIP6 (bottom) GCMs compared to ERA5 averaged over three European regions, from top to bottom: Northern Europe (NEU), Western & Central Europe (WCE) and Mediterranean (MED). The biases for each region and model are given with a number and shaded with colors according to the color bars to the right.

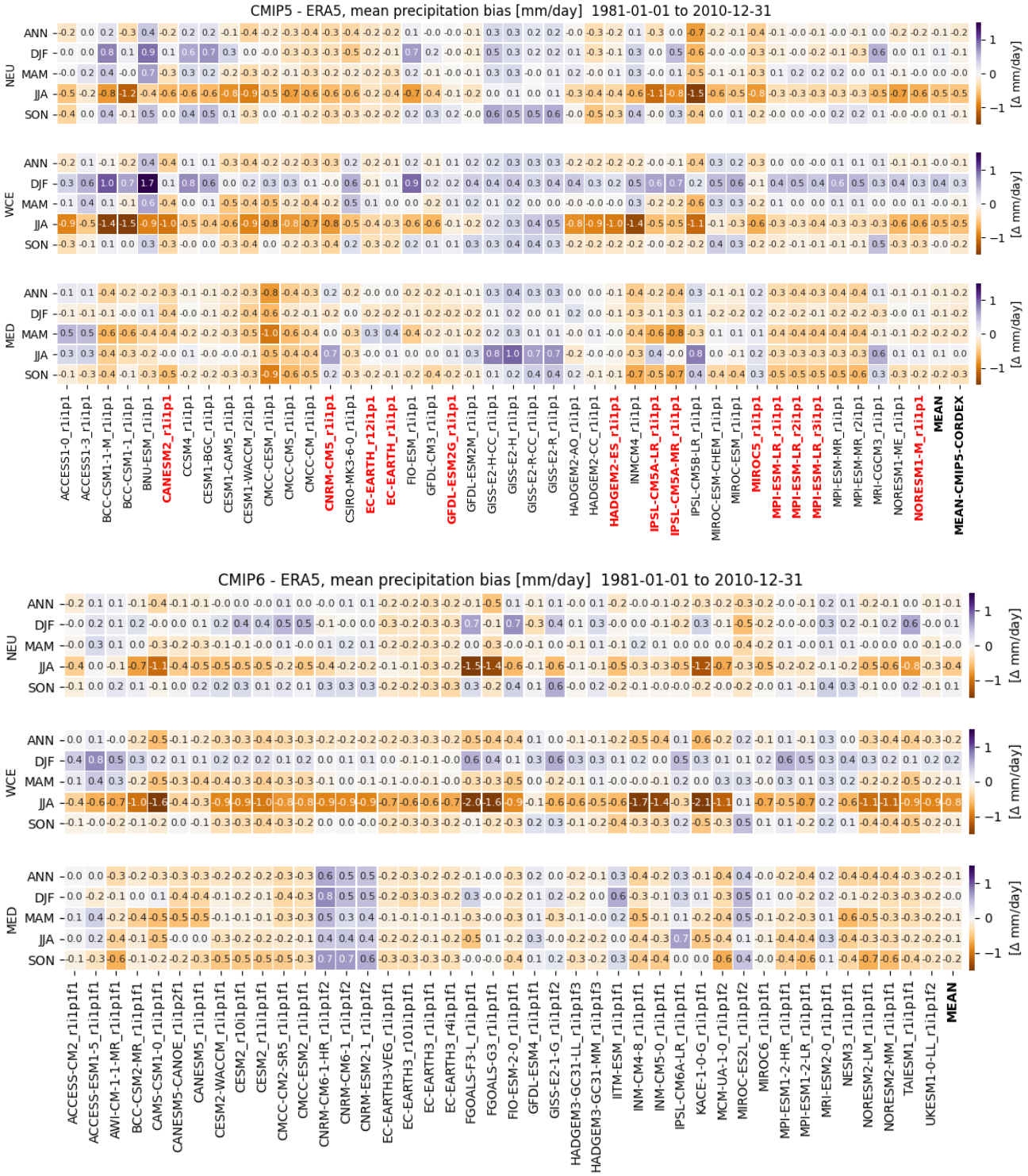

Figure A2.2. 30-year annual mean and seasonal mean precipitation bias (1981-2010) of CMIP5 (top), the CMIP5 GCMs used as forcing for the EURO-CORDEX RCMs are highlighted in red and CMIP6 (bottom) GCMs compared to ERA5 averaged 3 European regions, from top to bottom: Northern Europe (NEU), Western & Central Europe (WCE) and Mediterranean (MED). The biases for each region and model are given with a number and shaded with colors according to the color bars to the right.

3. Temperature change

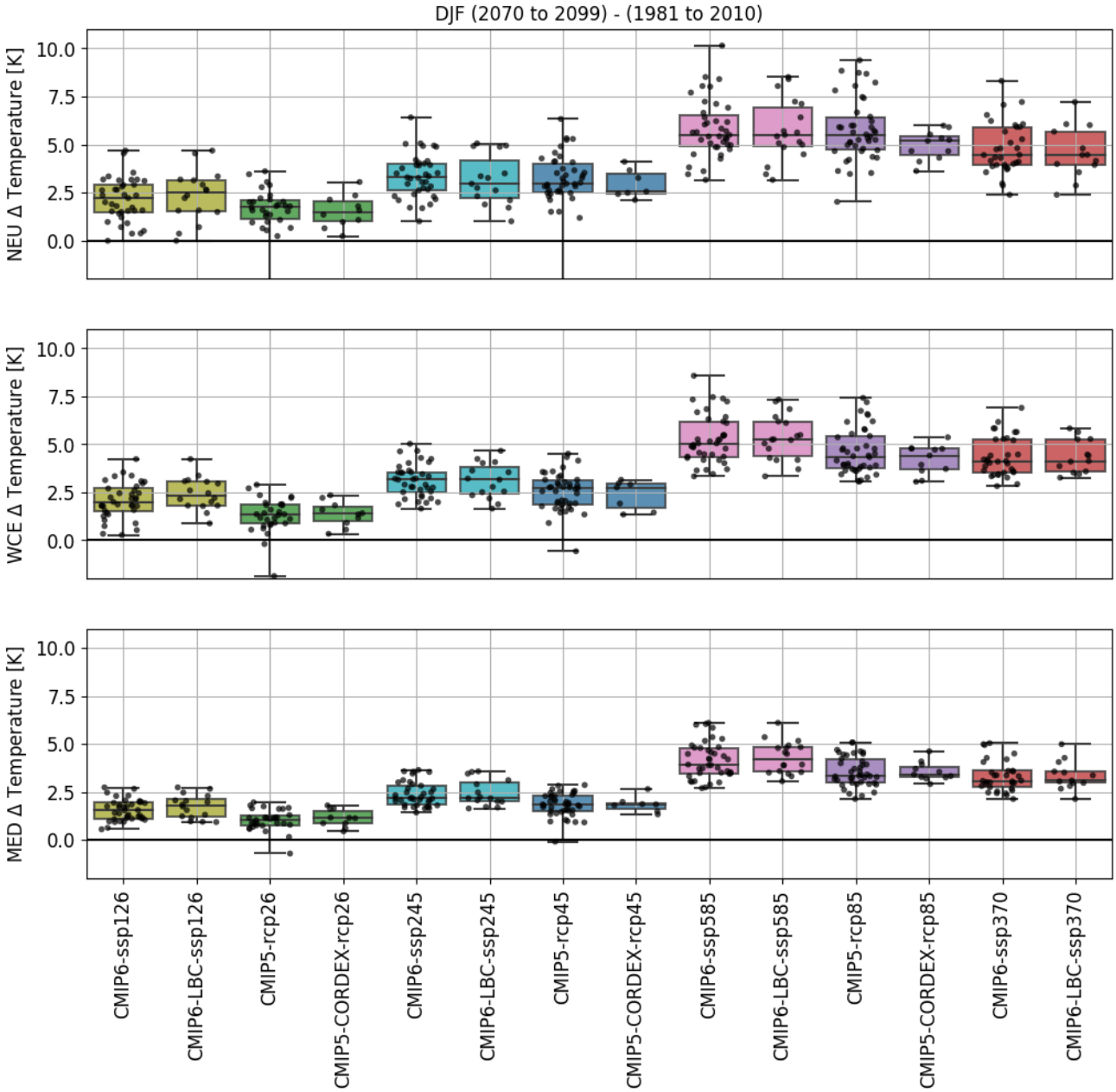

Figure A3.1. 30-year winter (DJF) mean temperature change (2070-2099) - (1981-2010) for scenario SSP1-2.6, SSP2-4.5, SSP5-8.5, SSP3-7.0 (lighter colors: lime, cyan, pink, red) and scenario RCP2.6, RCP4.5, RCP8.5 (darker colors: green, blue, purple) averaged over three European regions, from top to bottom: Northern Europe (NEU), Western & Central Europe (WCE) and Mediterranean (MED). Colored boxes present the ensemble spread between the 25th and 75th quantile for each ensemble: CMIP6, CMIP6-LBC (provide boundary data for dynamical downscaling), CMIP5 and CMIP5-CORDEX (used as forcing within EURO-CORDEX). The black bars present the ensemble minimum, median and maximum. The black dots represent the result of each single model of the ensemble.

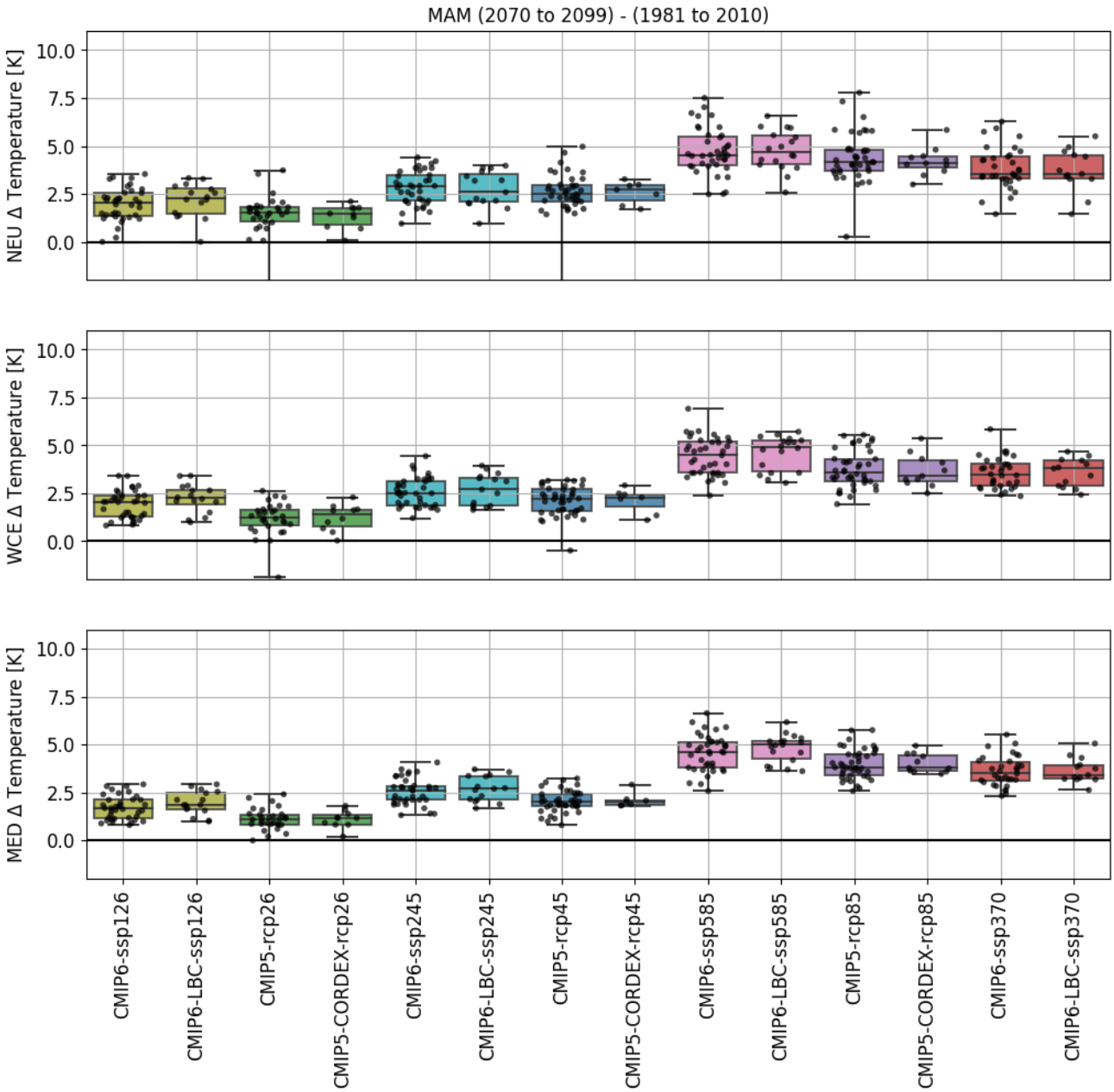

Figure A3.2. 30-year spring (MAM) mean temperature change (2070-2099) - (1981-2010) for scenario SSP1-2.6, SSP2-4.5, SSP5-8.5, SSP3-7.0 (lighter colors: lime, cyan, pink, red) and scenario RCP2.6, RCP4.5, RCP8.5 (darker colors: green, blue, purple) averaged over three European regions, from top to bottom: Northern Europe (NEU), Western & Central Europe (WCE) and Mediterranean (MED). Colored boxes present the ensemble spread between the 25th and 75th quantile for each ensemble: CMIP6, CMIP6-LBC (provide boundary data for dynamical downscaling), CMIP5 and CMIP5-CORDEX (used as forcing within EURO-CORDEX). The black bars present the ensemble minimum, median and maximum. The black dots represent the result of each single model of the ensemble.

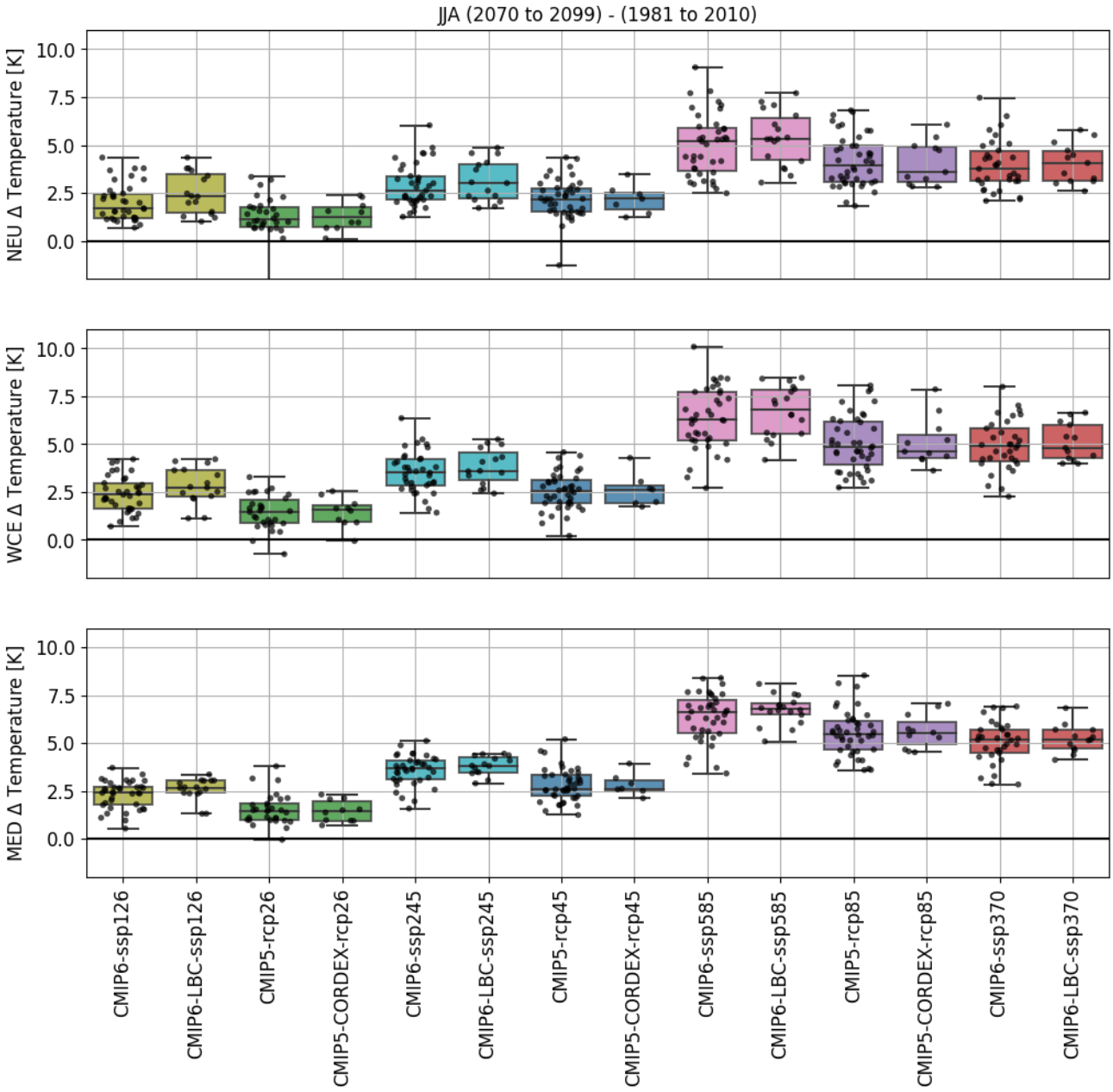

Figure A3.3. 30-year summer (JJA) mean temperature change (2070-2099) - (1981-2010) for scenario SSP1-2.6, SSP2-4.5, SSP5-8.5, SSP3-7.0 (lighter colors: lime, cyan, pink, red) and scenario RCP2.6, RCP4.5, RCP8.5 (darker colors: green, blue, purple) averaged over three European regions, from top to bottom: Northern Europe (NEU), Western & Central Europe (WCE) and Mediterranean (MED). Colored boxes present the ensemble spread between the 25th and 75th quantile for each ensemble: CMIP6, CMIP6-LBC (provide boundary data for dynamical downscaling), CMIP5 and CMIP5-CORDEX (used as forcing within EURO-CORDEX). The black bars present the ensemble minimum, median and maximum. The black dots represent the result of each single model of the ensemble.

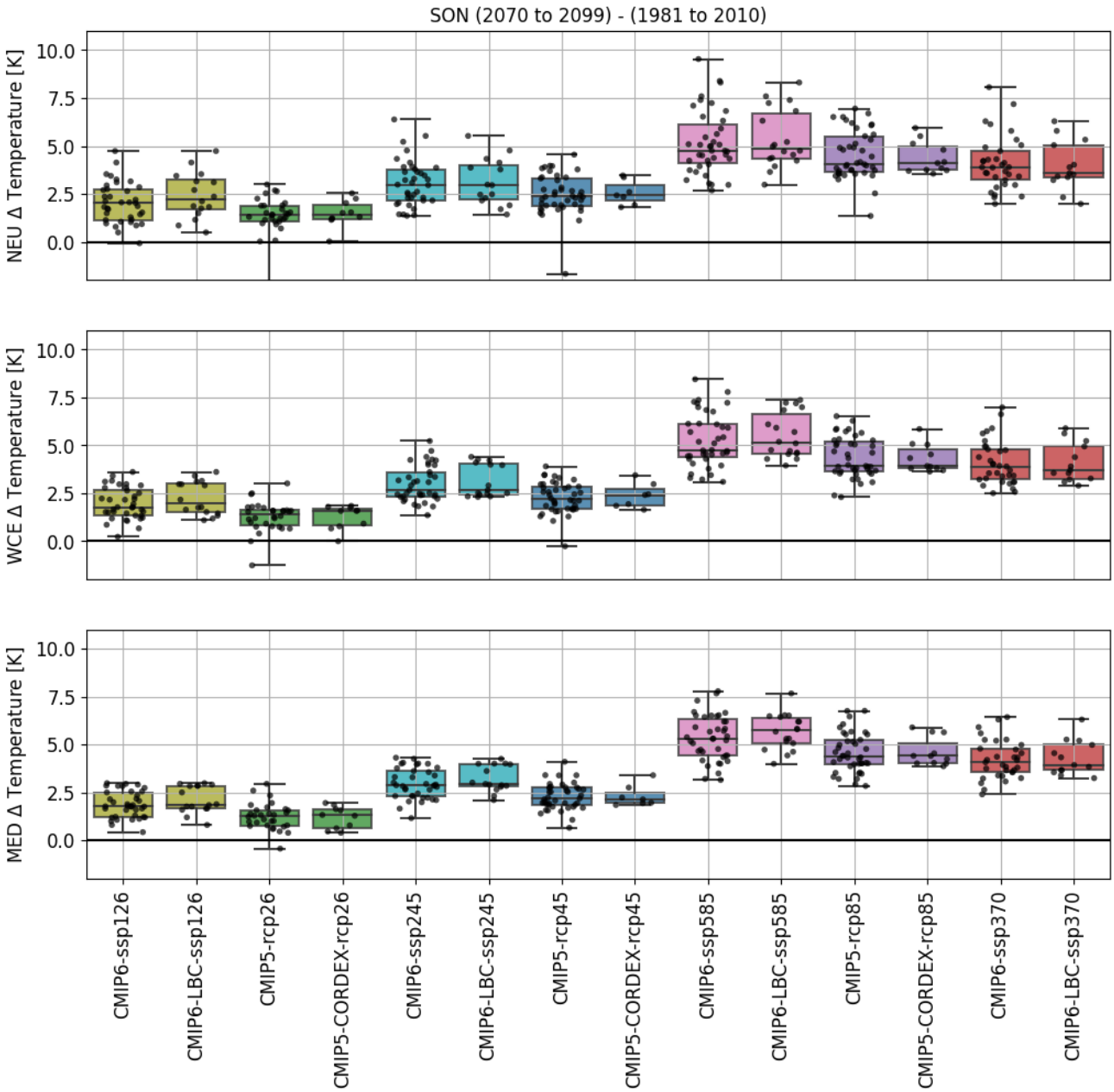

Figure A3.4. 30-year autumn (SON) mean temperature change (2070-2099) - (1981-2010) for scenario SSP1-2.6, SSP2-4.5, SSP5-8.5, SSP3-7.0 (lighter colors: lime, cyan, pink, red) and scenario RCP2.6, RCP4.5, RCP8.5 (darker colors: green, blue, purple) averaged over three European regions, from top to bottom: Northern Europe (NEU), Western & Central Europe (WCE) and Mediterranean (MED). Colored boxes present the ensemble spread between the 25th and 75th quantile for each ensemble: CMIP6, CMIP6-LBC (provide boundary data for dynamical downscaling), CMIP5 and CMIP5-CORDEX (used as forcing within EURO-CORDEX). The black bars present the ensemble minimum, median and maximum. The black dots represent the result of each single model of the ensemble.

4. Precipitation changes

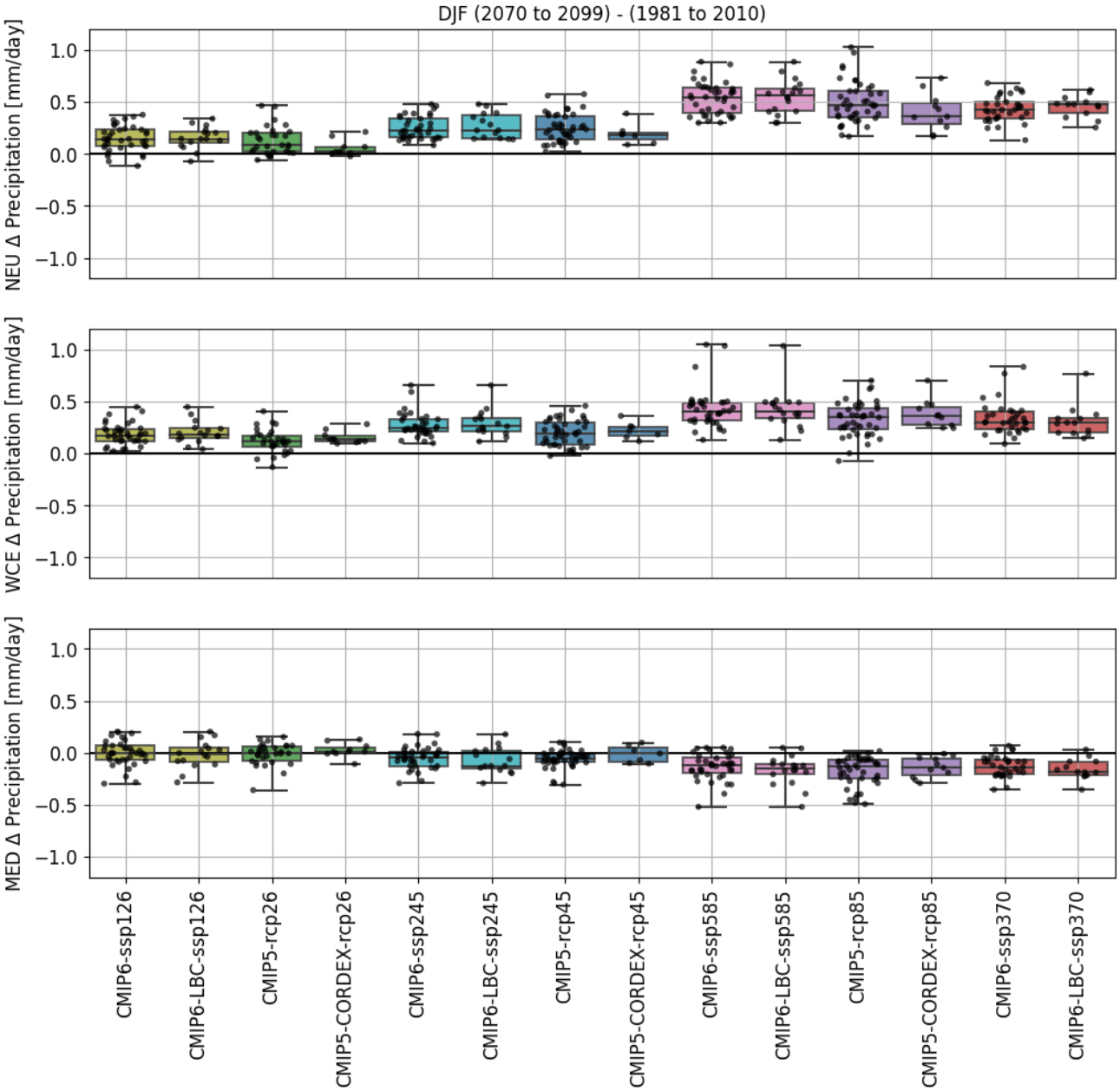

Figure A4.1. 30-year winter (DJF) mean precipitation change (2070-2099) - (1981-2010) for scenario SSP1-2.6, SSP2-4.5, SSP5-8.5, SSP3-7.0 (lighter colors: lime, cyan, pink, red) and scenario RCP2.6, RCP4.5, RCP8.5 (darker colors: green, blue, purple) averaged over three European regions, from top to bottom: Northern Europe (NEU), Western & Central Europe (WCE) and Mediterranean (MED). Colored boxes present the ensemble spread between the 25th and 75th quantile for each ensemble: CMIP6, CMIP6-LBC (provide boundary data for dynamical downscaling), CMIP5 and CMIP5-CORDEX (used as forcing within EURO-CORDEX). The black bars present the ensemble minimum, median and maximum. The black dots represent the result of each single model of the ensemble.

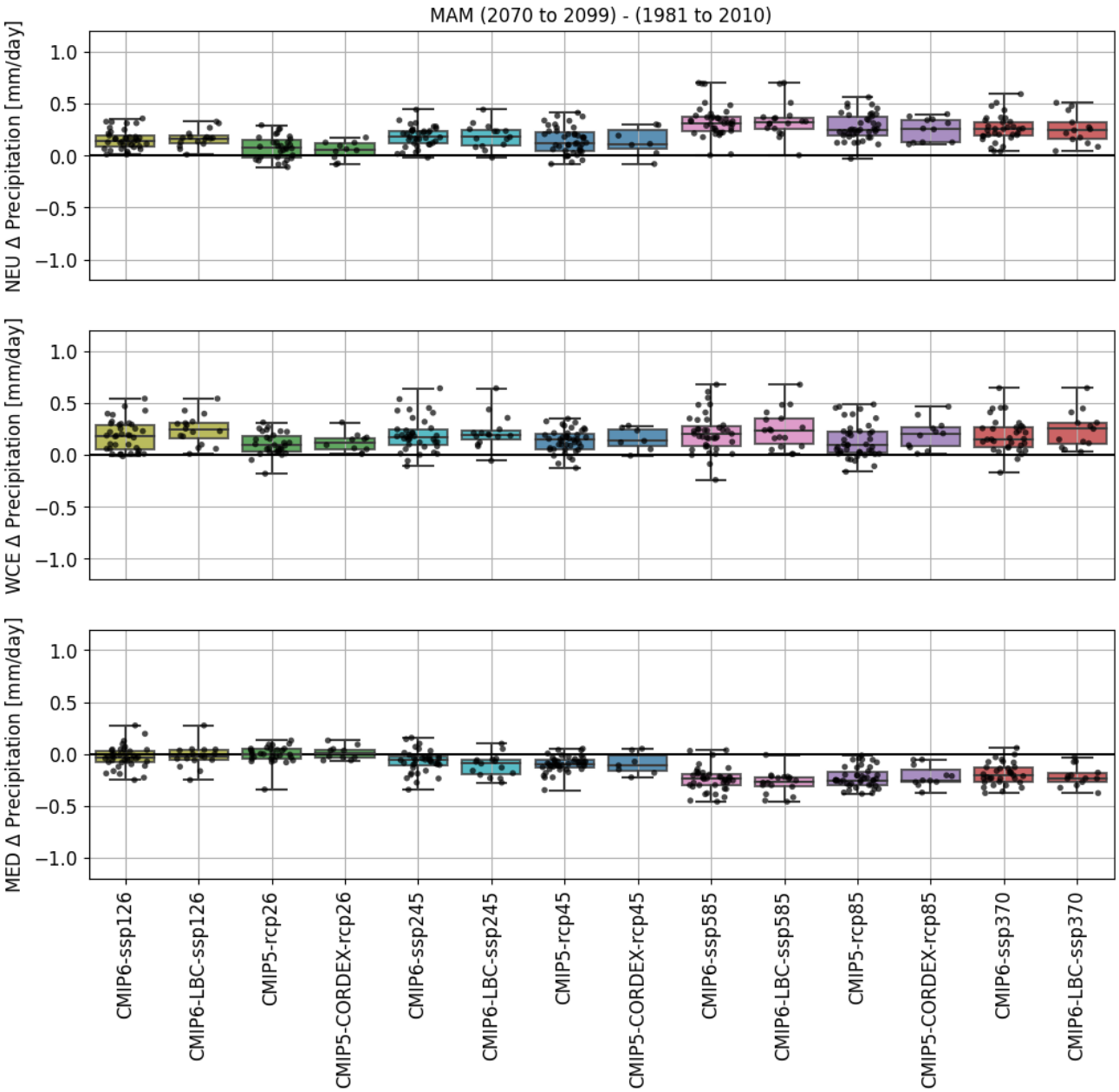

Figure A4.2. 30-year spring (MAM) mean precipitation change (2070-2099) - (1981-2010) for scenario SSP1-2.6, SSP2-4.5, SSP5-8.5, SSP3-7.0 (lighter colors: lime, cyan, pink, red) and scenario RCP2.6, RCP4.5, RCP8.5 (darker colors: green, blue, purple) averaged over three European regions, from top to bottom: Northern Europe (NEU), Western & Central Europe (WCE) and Mediterranean (MED). Colored boxes present the ensemble spread between the 25th and 75th quantile for each ensemble: CMIP6, CMIP6-LBC (provide boundary data for dynamical downscaling), CMIP5 and CMIP5-CORDEX (used as forcing within EURO-CORDEX). The black bars present the ensemble minimum, median and maximum. The black dots represent the result of each single model of the ensemble.

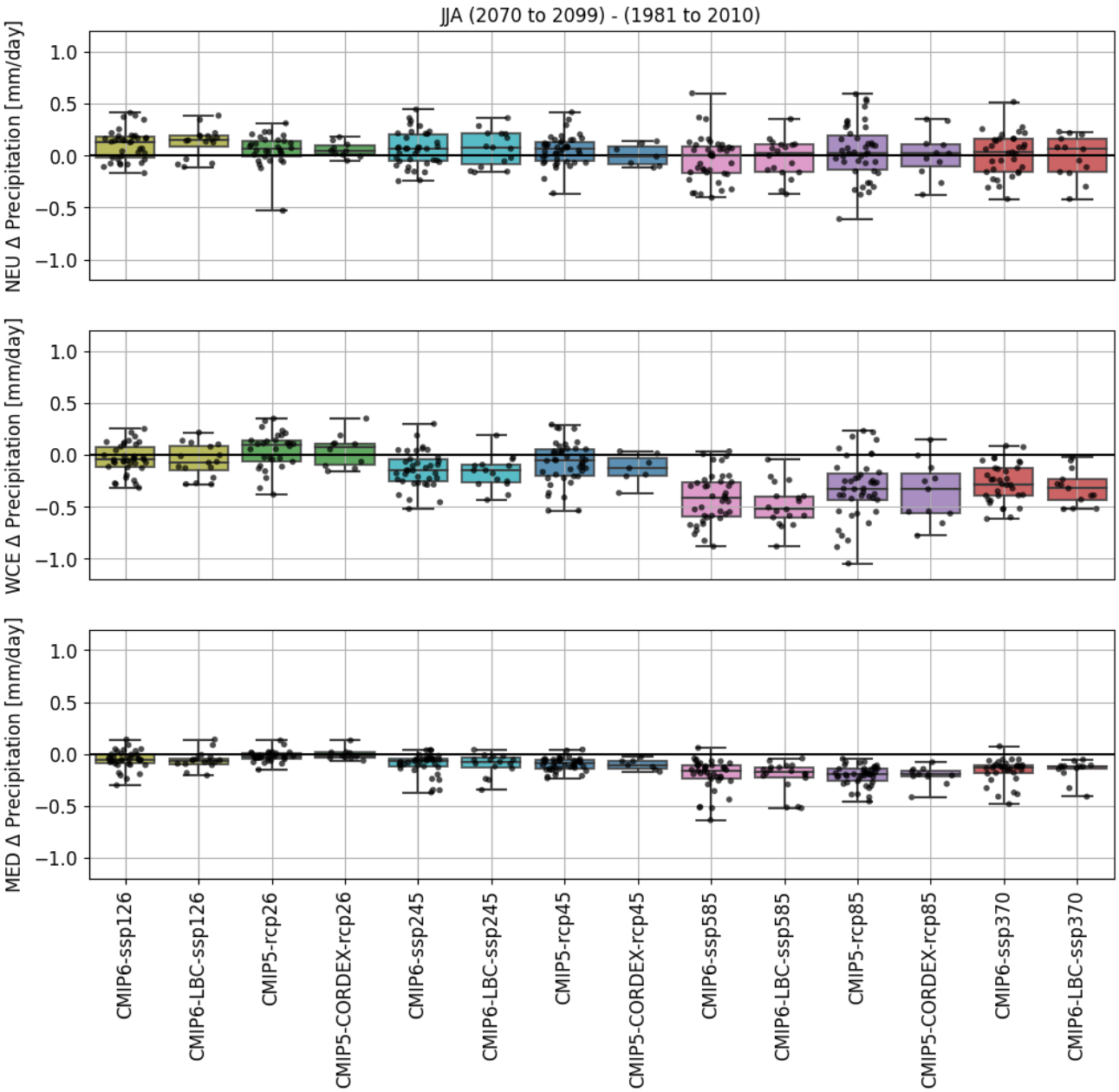

Figure A4.3. 30-year summer (JJA) mean precipitation change (2070-2099) - (1981-2010) for scenario SSP1-2.6, SSP2-4.5, SSP5-8.5, SSP3-7.0 (lighter colors: lime, cyan, pink, red) and scenario RCP2.6, RCP4.5, RCP8.5 (darker colors: green, blue, purple) averaged over three European regions, from top to bottom: Northern Europe (NEU), Western & Central Europe (WCE) and Mediterranean (MED). Colored boxes present the ensemble spread between the 25th and 75th quantile for each ensemble: CMIP6, CMIP6-LBC (provide boundary data for dynamical downscaling), CMIP5 and CMIP5-CORDEX (used as forcing within EURO-CORDEX). The black bars present the ensemble minimum, median and maximum. The black dots represent the result of each single model of the ensemble.

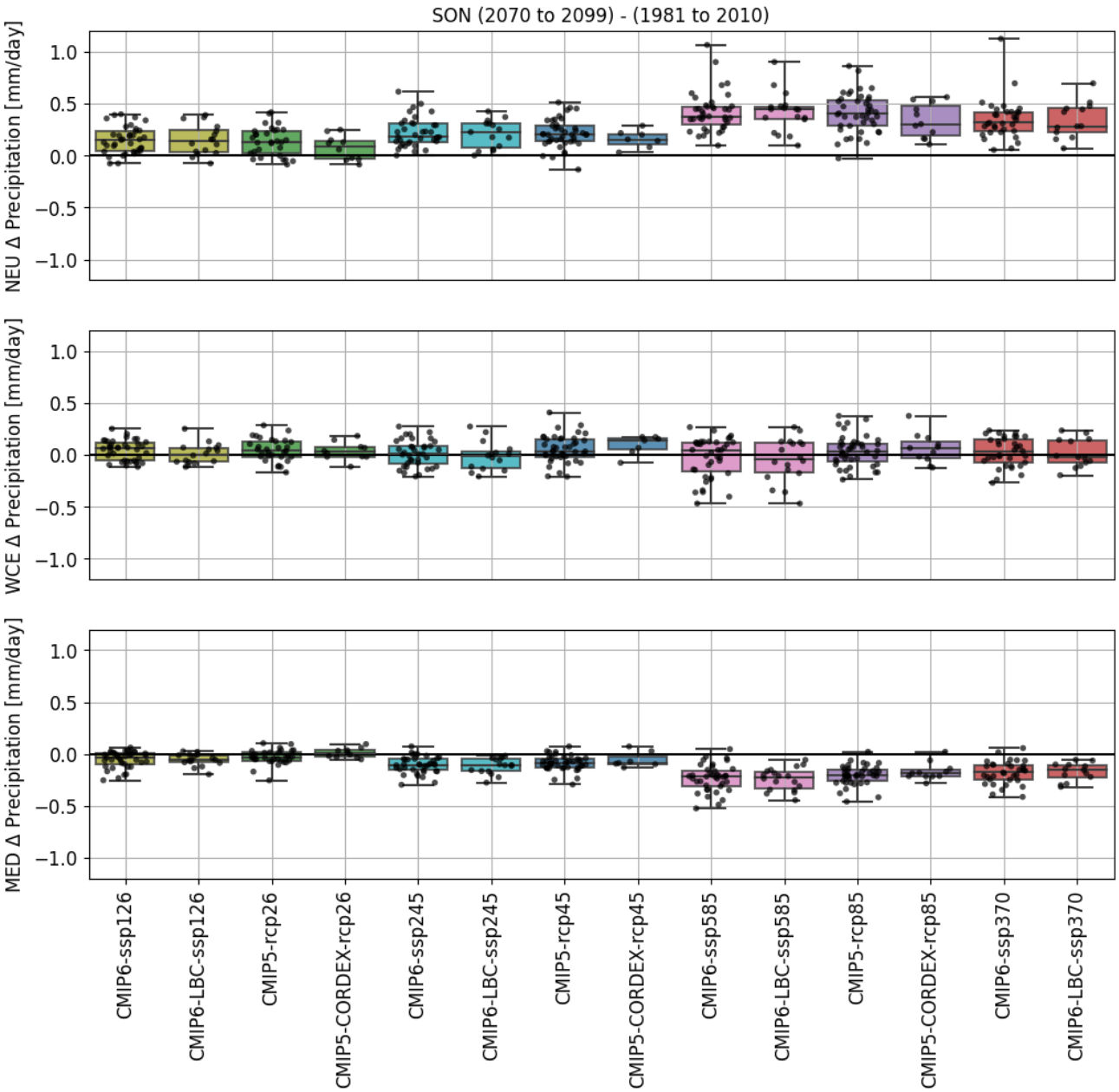

Figure A4.4. 30-year autumn (SON) mean precipitation change (2070-2099) - (1981-2010) for scenario SSP1-2.6, SSP2-4.5, SSP5-8.5, SSP3-7.0 (lighter colors: lime, cyan, pink, red) and scenario RCP2.6, RCP4.5, RCP8.5 (darker colors: green, blue, purple) averaged over three European regions, from top to bottom: Northern Europe (NEU), Western & Central Europe (WCE) and Mediterranean (MED). Colored boxes present the ensemble spread between the 25th and 75th quantile for each ensemble: CMIP6, CMIP6-LBC (provide boundary data for dynamical downscaling), CMIP5 and CMIP5-CORDEX (used as forcing within EURO-CORDEX). The black bars present the ensemble minimum, median and maximum. The black dots represent the result of each single model of the ensemble.

5. Temperature and precipitation change

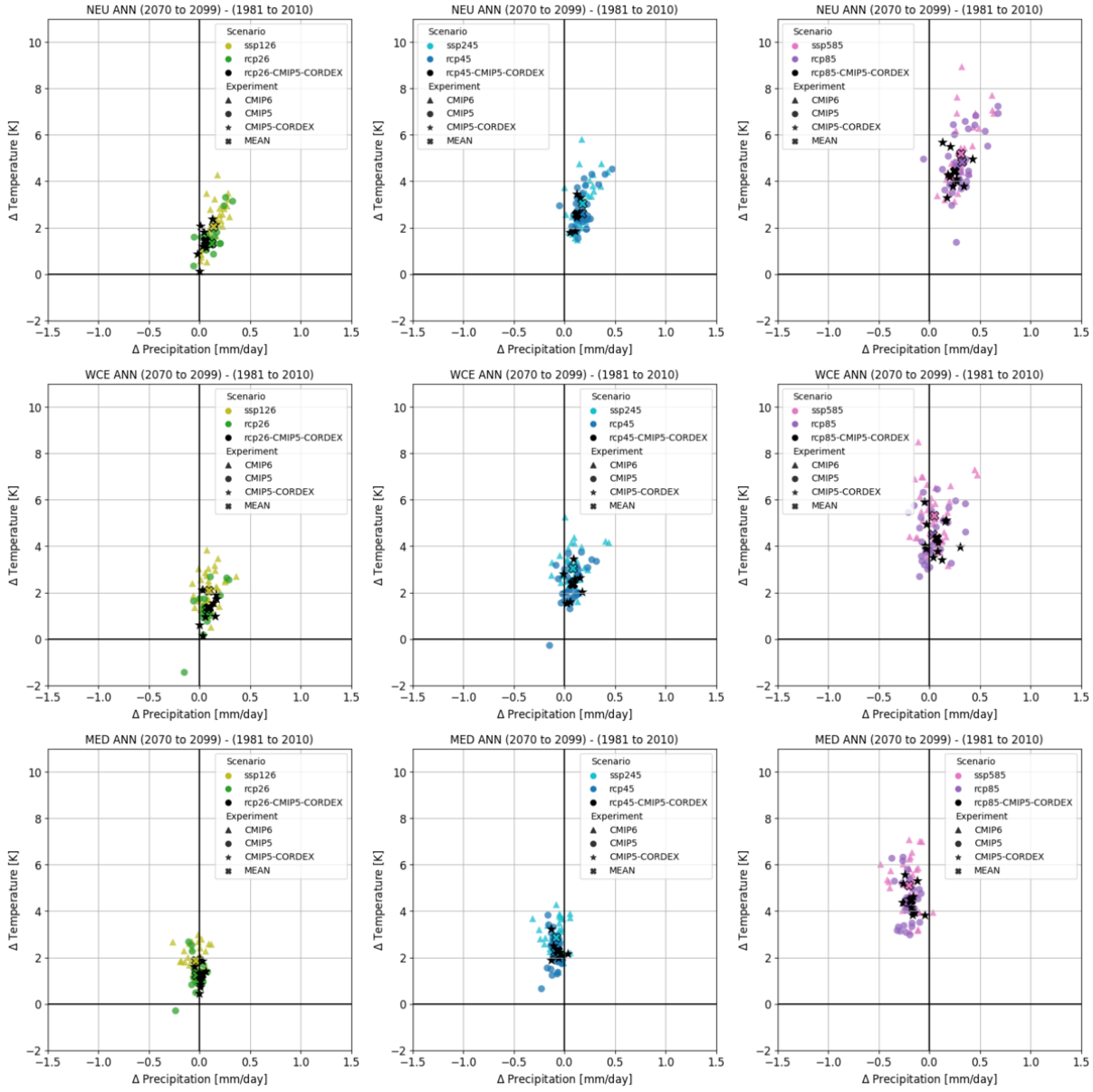

Figure A5.1. 30-year mean annual temperature and precipitation change (2070 to 2099) – (1981 to 2010) calculated by the GCMs from CMIP5 (triangles) and CMIP6 (circles) with color coding according to the different scenarios. From left to right: RCP2.6/SSP1-2.6, RCP4.5/SSP2-4.5, RCP8.5/SSP5-8.5. The CMIP5 GCMs used as forcing for the EURO-CORDEX RCMs are marked by black stars in all panels. From top to bottom the regions: Northern Europe (NEU), Western & Central Europe (WCE) and Mediterranean (MED).

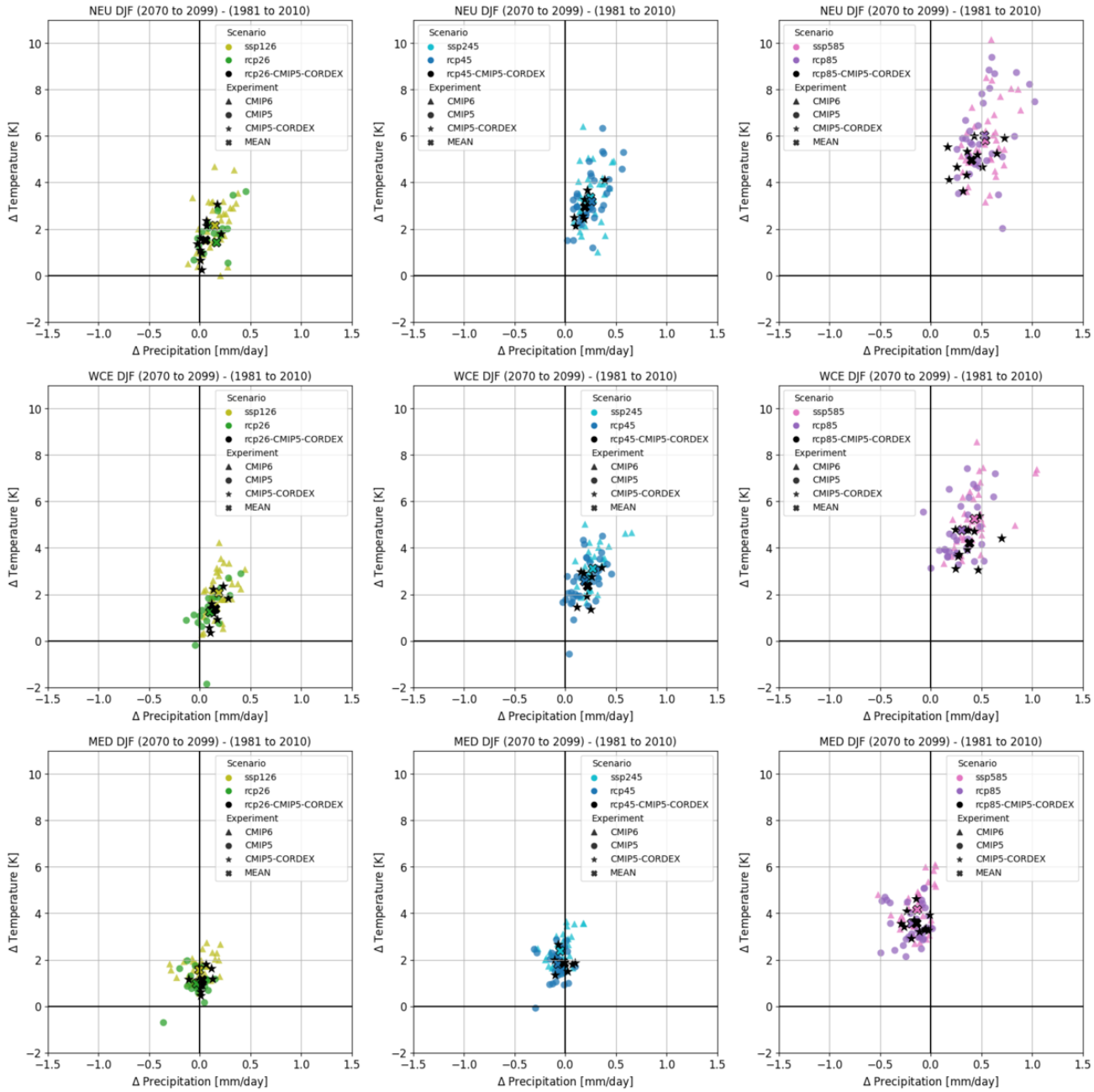

Figure A5.2. 30-year mean winter (DJF) temperature and precipitation change (2070 to 2099) – (1981 to 2010) calculated by the GCMs from CMIP5 (triangles) and CMIP6 (circles) with color coding according to the different scenarios. From left to right: RCP2.6/SSP1-2.6, RCP4.5/SSP2-4.5, RCP8.5/SSP5-8.5. The CMIP5 GCMs used as forcing for the EURO-CORDEX RCMs are marked by black stars in all panels. From top to bottom the regions: Northern Europe (NEU), Western & Central Europe (WCE) and Mediterranean (MED).

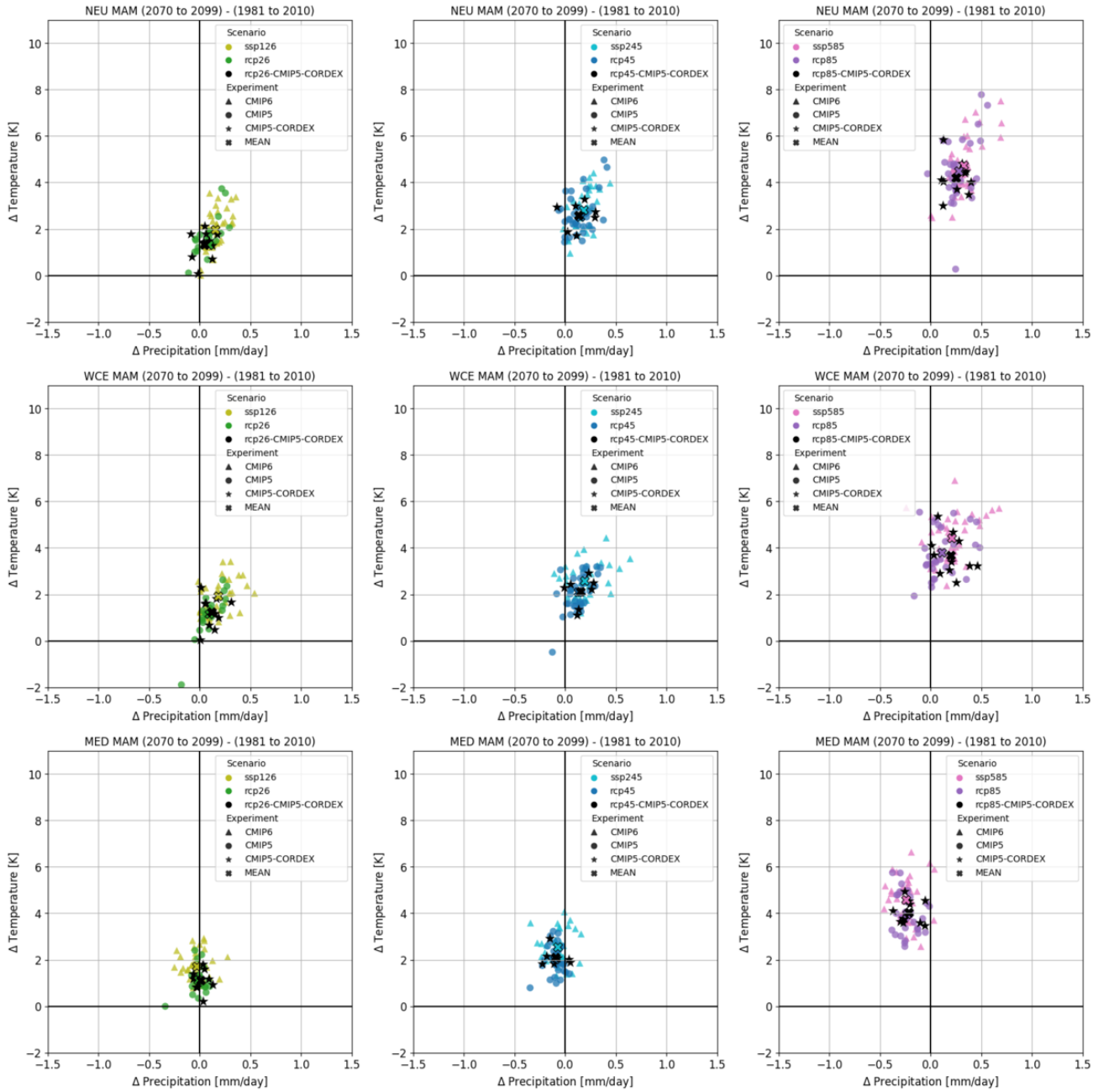

Figure A5.3. 30-year mean spring (MAM) temperature and precipitation change (2070 to 2099) – (1981 to 2010) calculated by the GCMs from CMIP5 (triangles) and CMIP6 (circles) with color coding according to the different scenarios. From left to right: RCP2.6/SSP1-2.6, RCP4.5/SSP2-4.5, RCP8.5/SSP5-8.5. The CMIP5 GCMs used as forcing for the EURO-CORDEX RCMs are marked by black stars in all panels. From top to bottom the regions: Northern Europe (NEU), Western & Central Europe (WCE) and Mediterranean (MED).

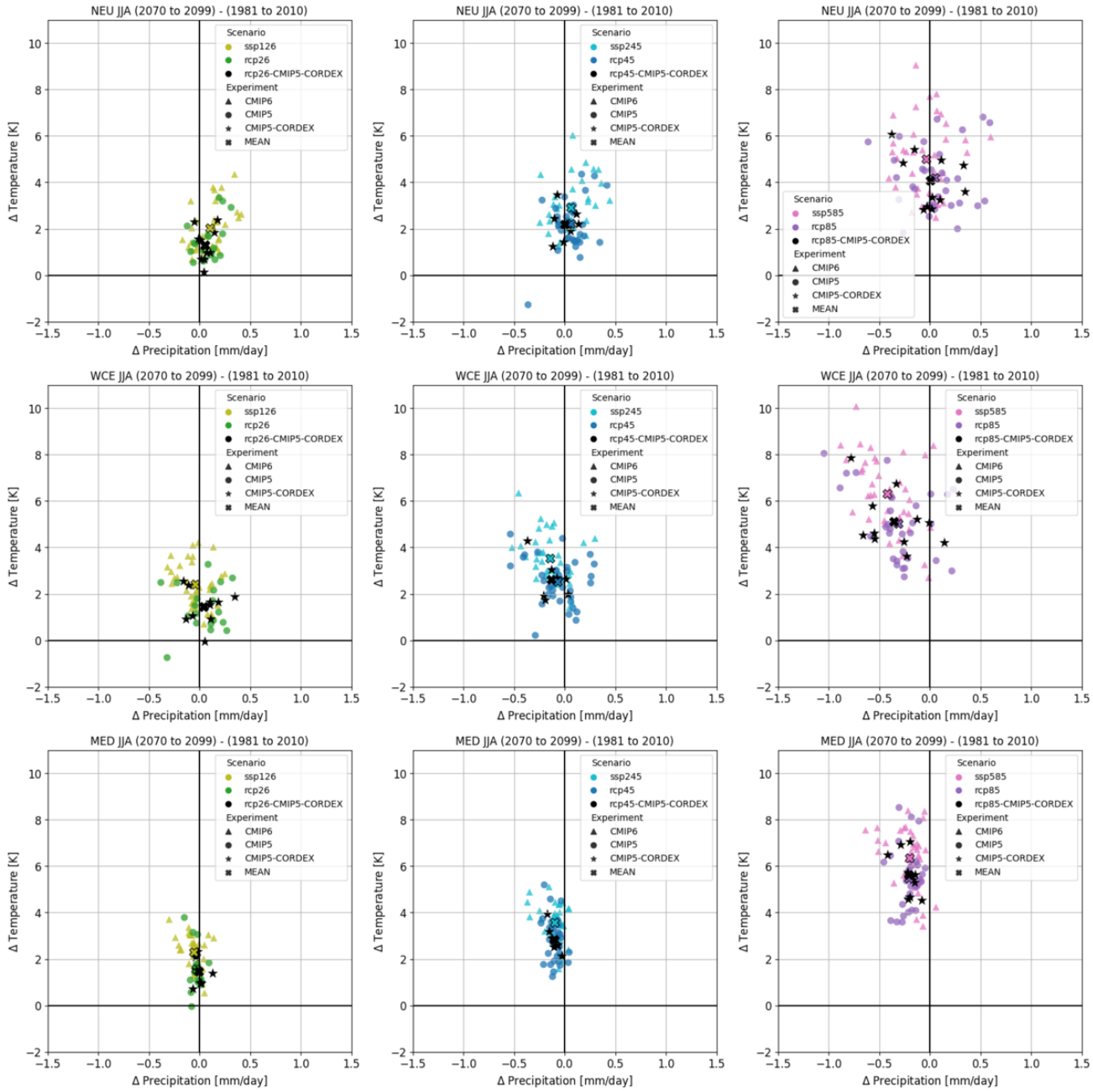

Figure A5.4. 30-year mean summer (JJA) temperature and precipitation change (2070 to 2099) – (1981 to 2010) calculated by the GCMs from CMIP5 (triangles) and CMIP6 (circles) with color coding according to the different scenarios. From left to right: RCP2.6/SSP1-2.6, RCP4.5/SSP2-4.5, RCP8.5/SSP5-8.5. The CMIP5 GCMs used as forcing for the EURO-CORDEX RCMs are marked by black stars in all panels. From top to bottom the regions: Northern Europe (NEU), Western & Central Europe (WCE) and Mediterranean (MED).

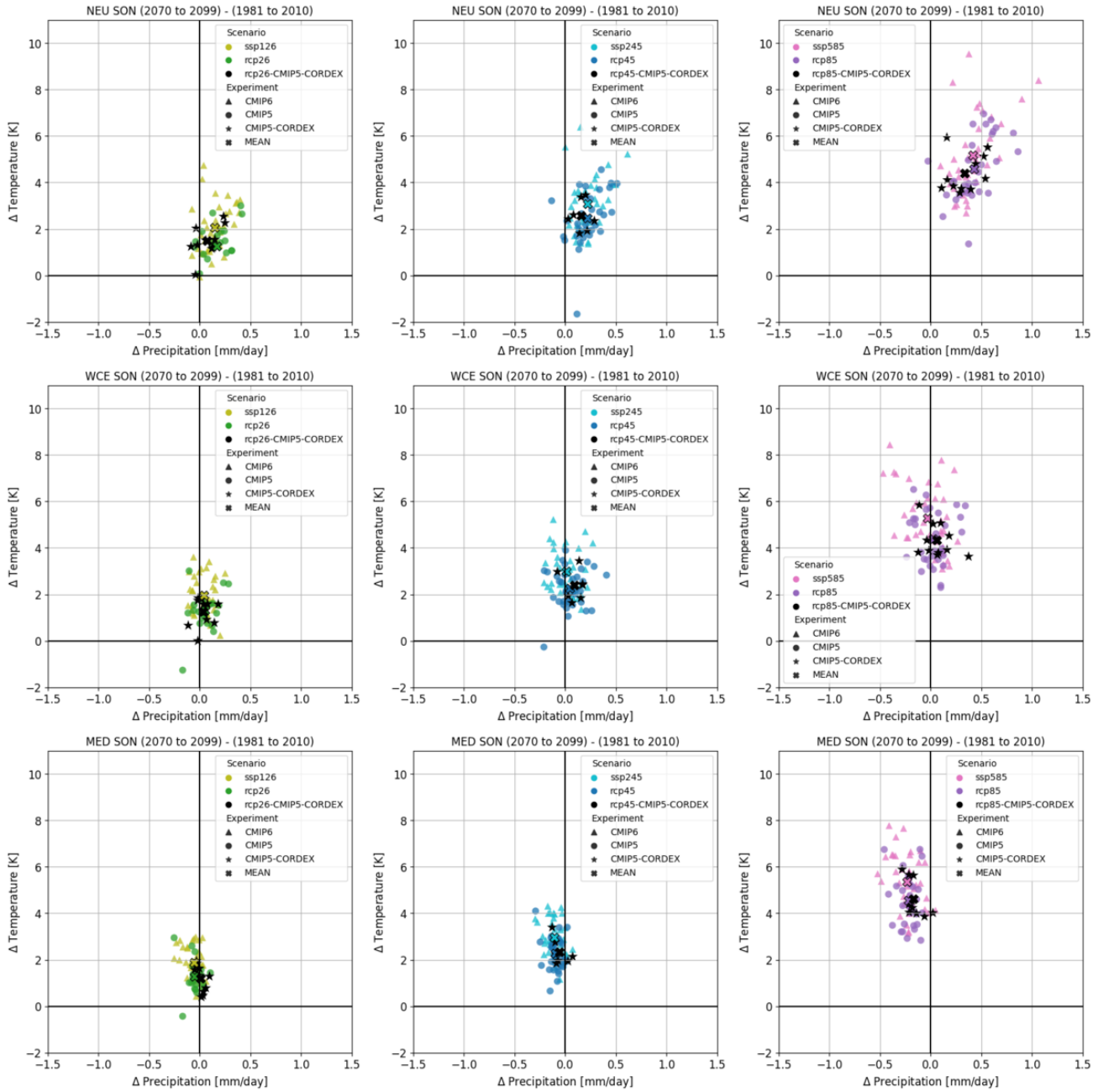

Figure A5.5. 30-year mean autumn (SON) temperature and precipitation change (2070 to 2099) – (1981 to 2010) calculated by the GCMs from CMIP5 (triangles) and CMIP6 (circles) with color coding according to the different scenarios. From left to right: RCP2.6/SSP1-2.6, RCP4.5/SSP2-4.5, RCP8.5/SSP5-8.5. The CMIP5 GCMs used as forcing for the EURO-CORDEX RCMs are marked by black stars in all panels. From top to bottom the regions: Northern Europe (NEU), Western & Central Europe (WCE) and Mediterranean (MED).

6. Mean annual cycle of temperature change

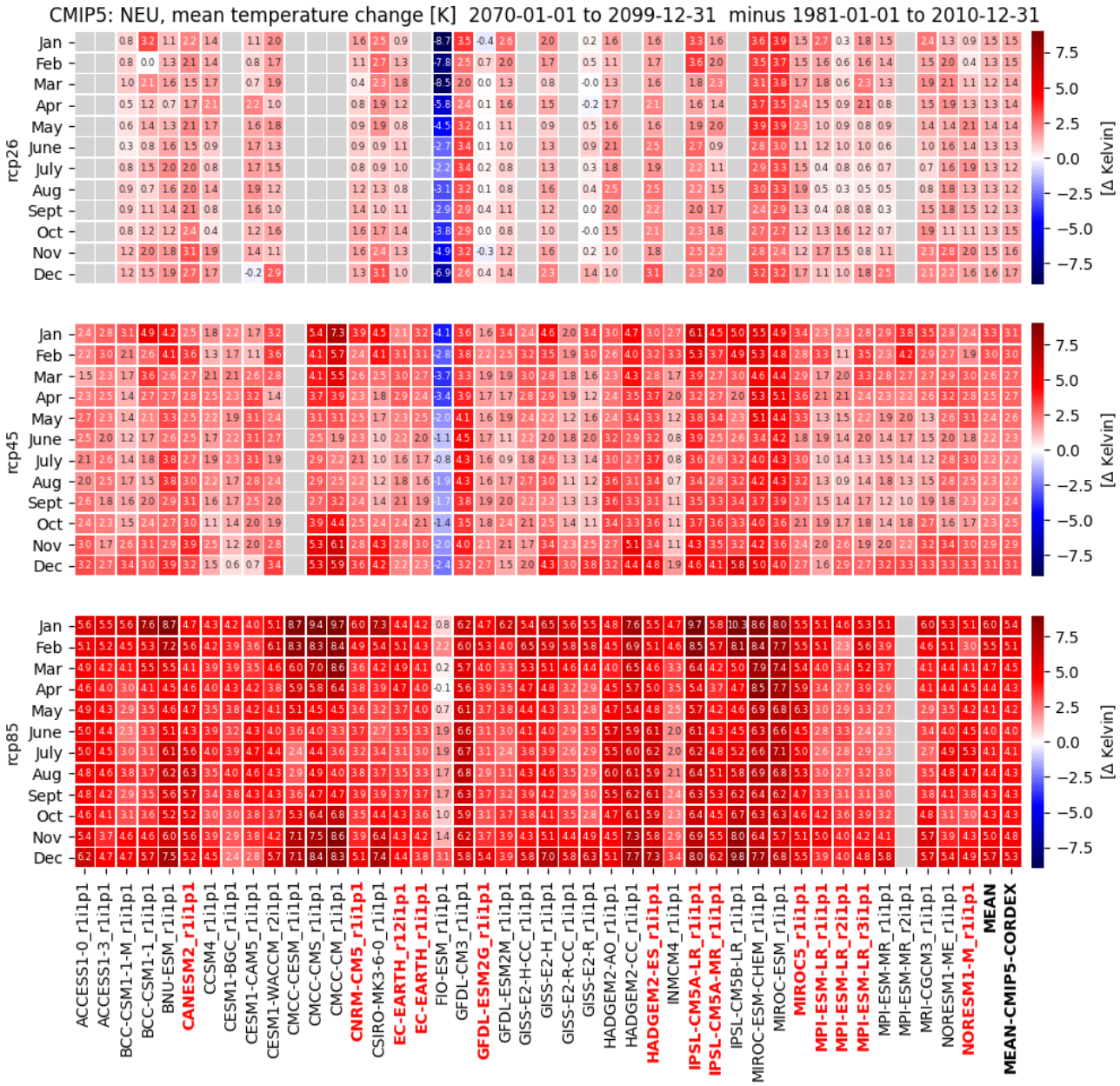

Figure A6.1. Northern Europe (NEU): 30-year mean annual cycle of temperature change (2070 to 2099) – (1981 to 2010) calculated by the GCMs from CMIP5, the CMIP5 GCMs used as forcing for the EURO-CORDEX RCMs are highlighted in red, from top to bottom: RCP2.6, RCP4.5, RCP8.5. The boxes are grey, if a simulation was not available. The changes for each region and model are given with a number and shaded with colors according to the color bars to the right.

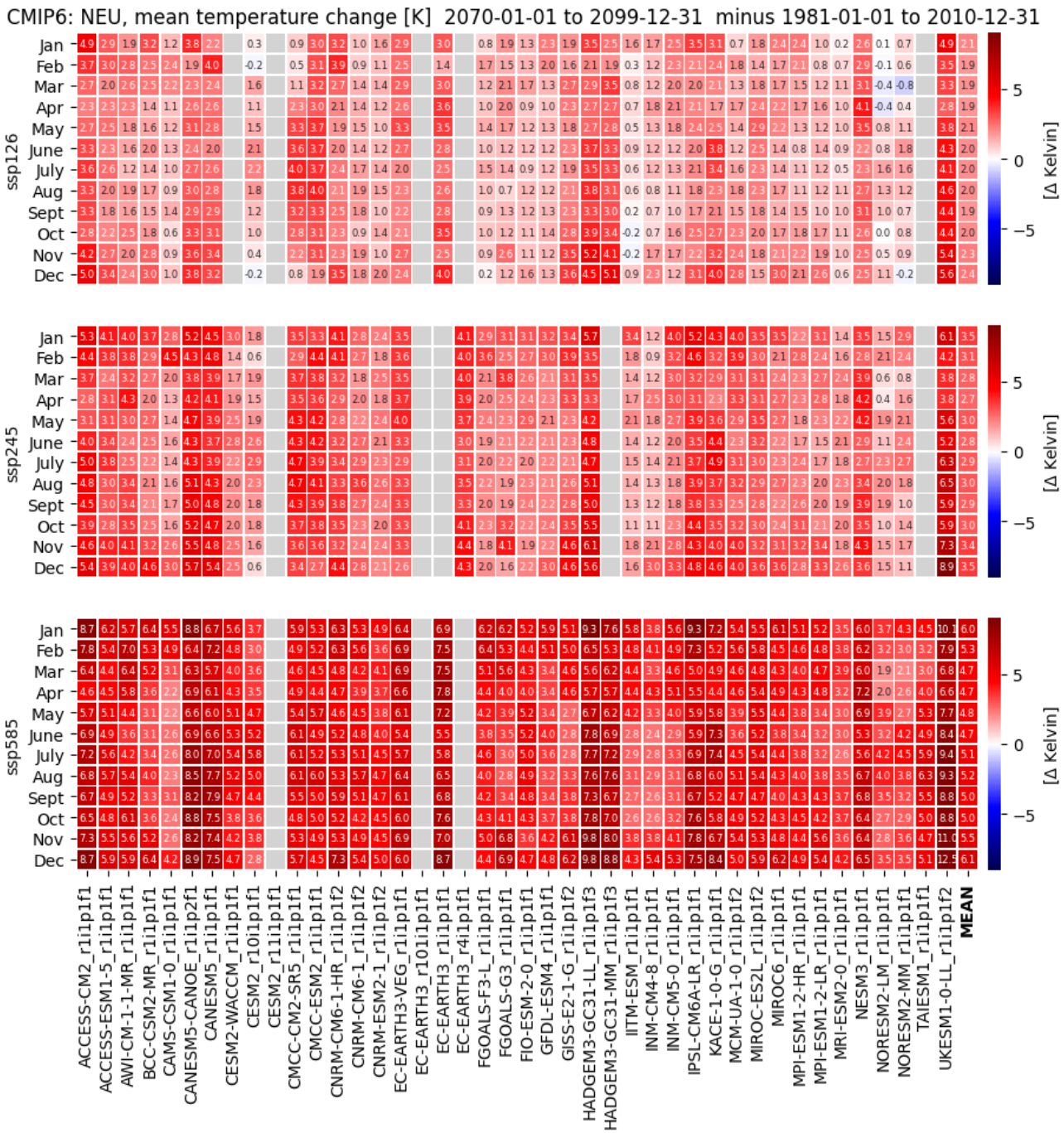

Figure A6.2. Northern Europe (NEU): 30-year mean annual cycle of temperature change (2070 to 2099) – (1981 to 2010) calculated by the GCMs from CMIP6, from top to bottom: SSP1-2.6, SSP2-4.5, SSP5-8.5. The boxes are grey, if a simulation was not available. The changes for each region and model are given with a number and shaded with colors according to the color bars to the right.

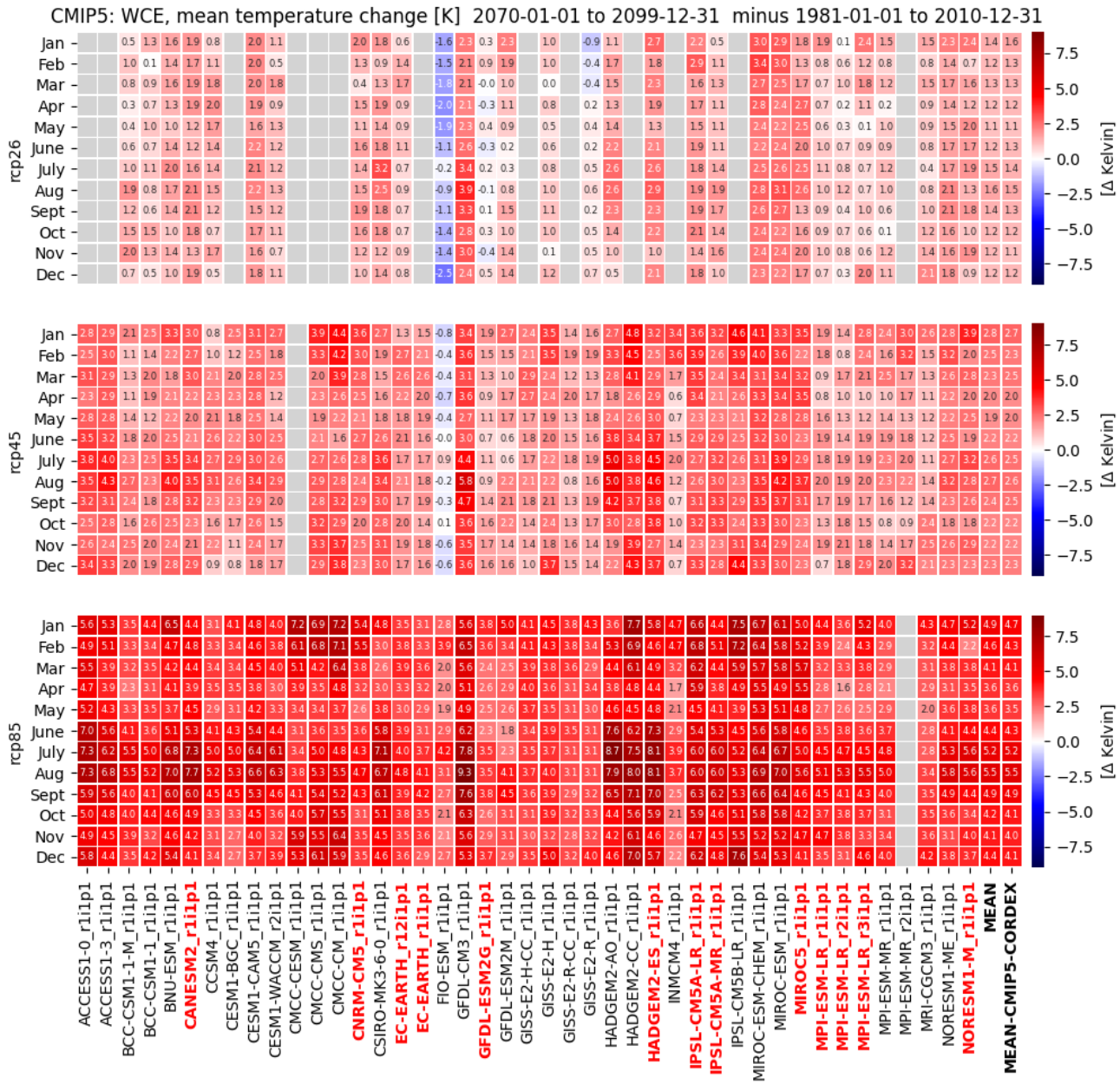

Figure A6.3. Western & Central Europe (WCE): 30-year mean annual cycle of temperature change (2070 to 2099) – (1981 to 2010) calculated by the GCMs from CMIP5, the CMIP5 GCMs used as forcing for the EURO-CORDEX RCMs are highlighted in red, from top to bottom: RCP2.6, RCP4.5, RCP8.5. The boxes are grey, if a simulation was not available. The changes for each region and model are given with a number and shaded with colors according to the color bars to the right.

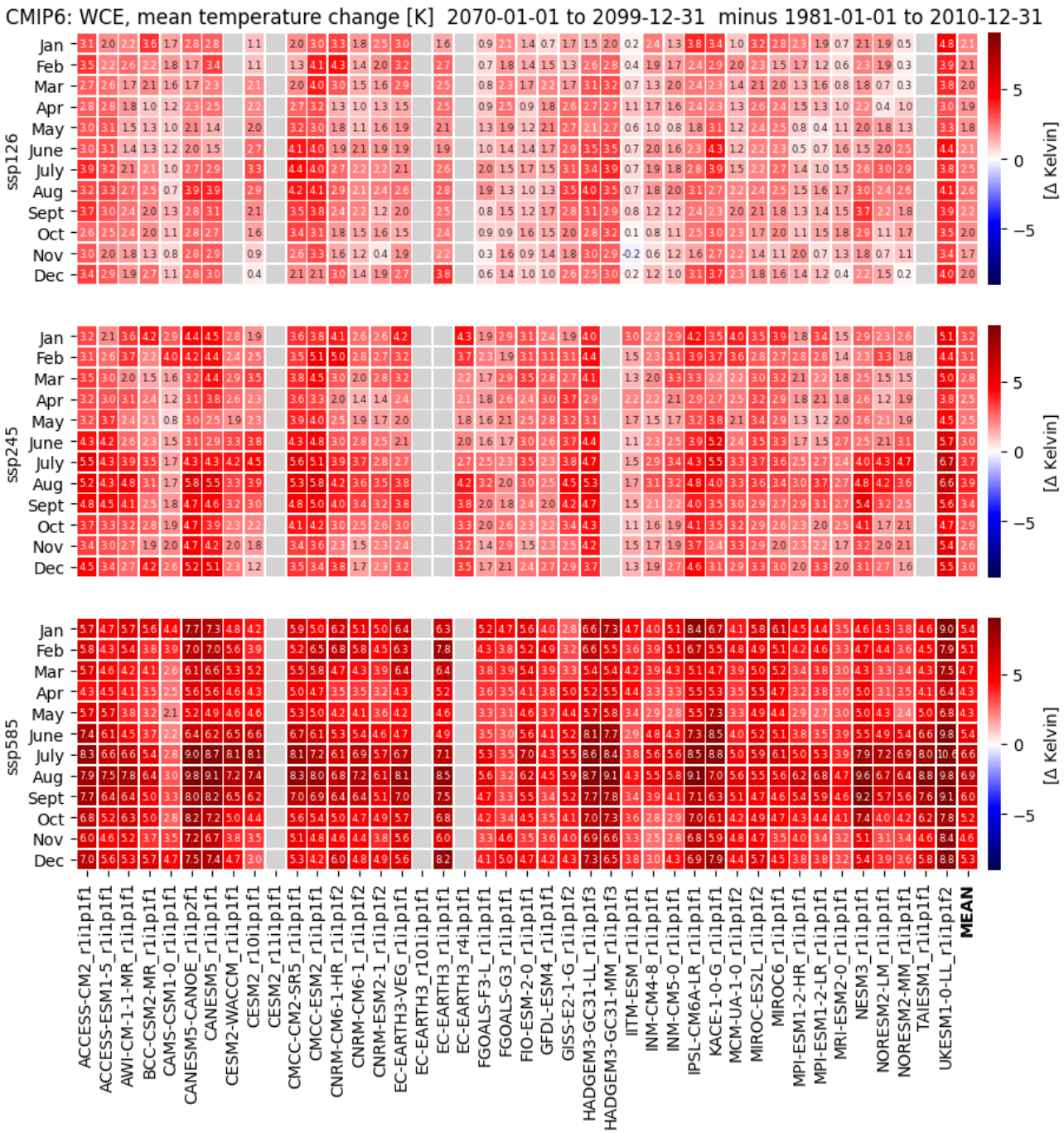

Figure A6.4. Western & Central Europe (WCE): 30-year mean annual cycle of temperature change (2070 to 2099) – (1981 to 2010) calculated by the GCMs from CMIP6, from top to bottom: SSP1-2.6, SSP2-4.5, SSP5-8.5. The boxes are grey, if a simulation was not available. The changes for each region and model are given with a number and shaded with colors according to the color bars to the right.

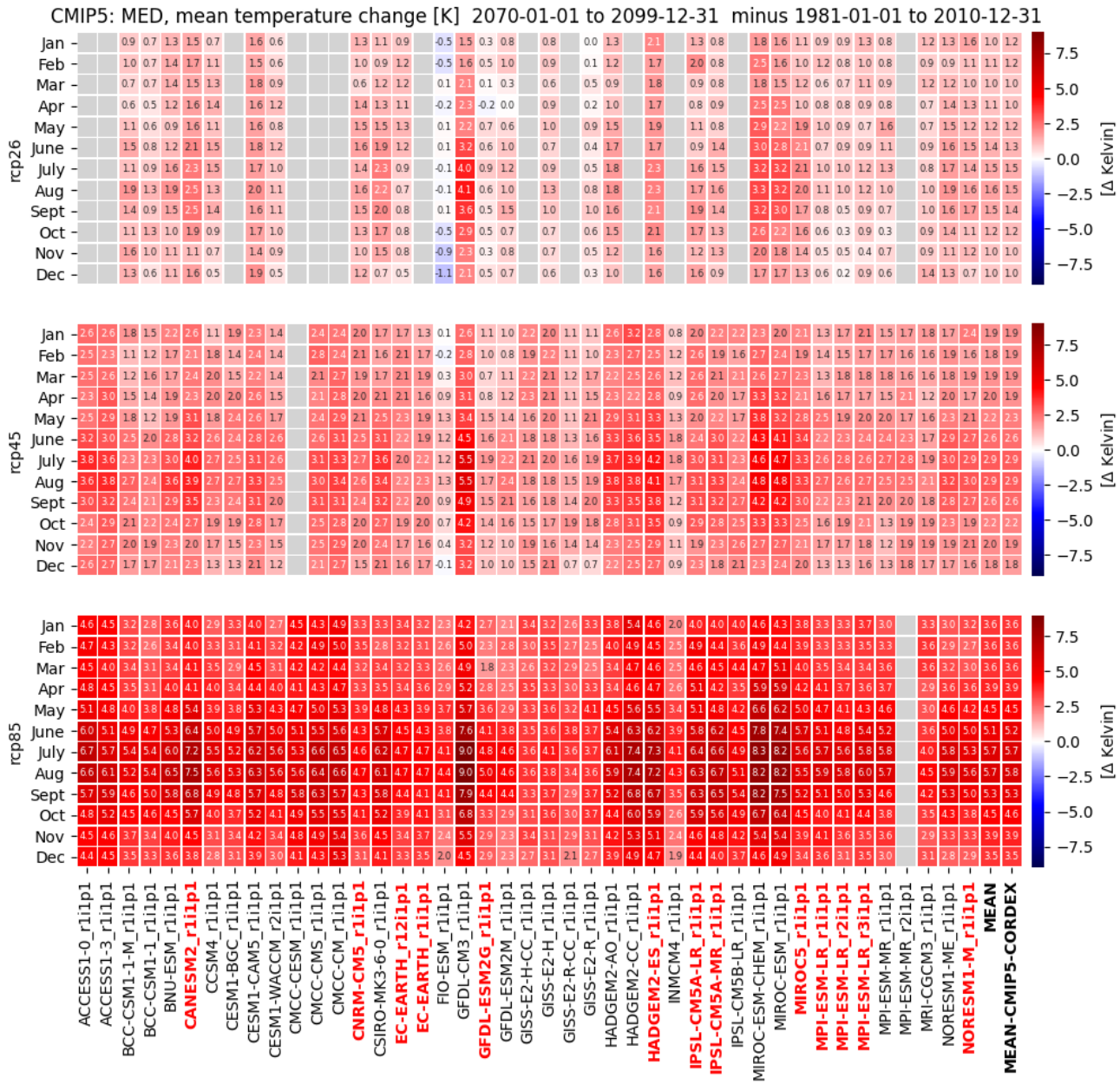

Figure A6.5. Mediterranean (MED): 30-year mean annual cycle of temperature change (2070 to 2099) – (1981 to 2010) calculated by the GCMs from CMIP5 and CMIP6, the CMIP5 GCMs used as forcing for the EURO-CORDEX RCMs are highlighted in red, from top to bottom: RCP2.6, RCP4.5, RCP8.5. The boxes are grey, if a simulation was not available. The changes for each region and model are given with a number and shaded with colors according to the color bars to the right.

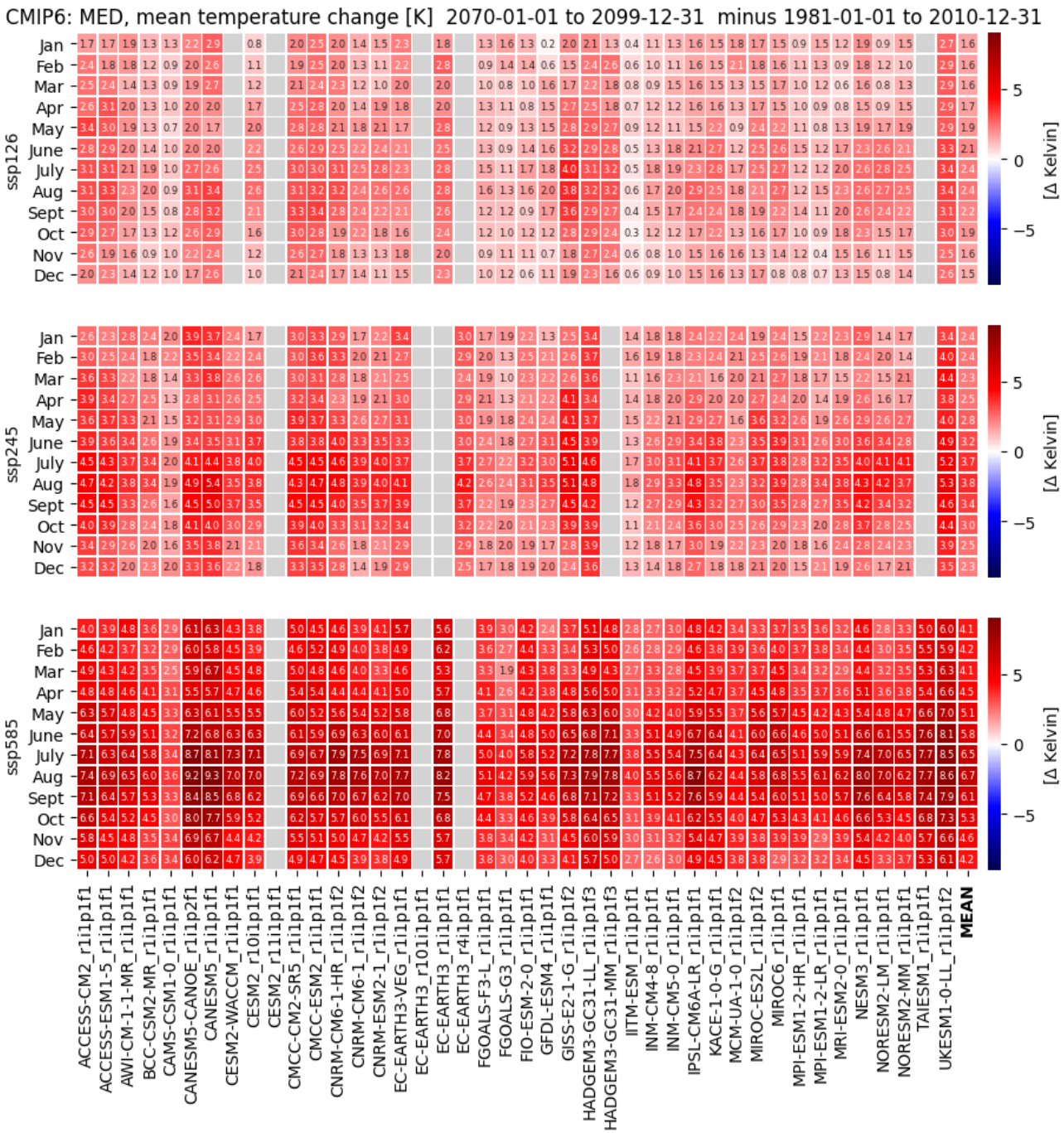

Figure A6.6. Mediterranean (MED): 30-year mean annual cycle of temperature change (2070 to 2099) – (1981 to 2010) calculated by the GCMs from CMIP6, from top to bottom: SSP1-2.6, SSP2-4.5, SSP5-8.5. The boxes are grey, if a simulation was not available. The changes for each region and model are given with a number and shaded with colors according to the color bars to the right.

7. Mean annual cycle of precipitation change

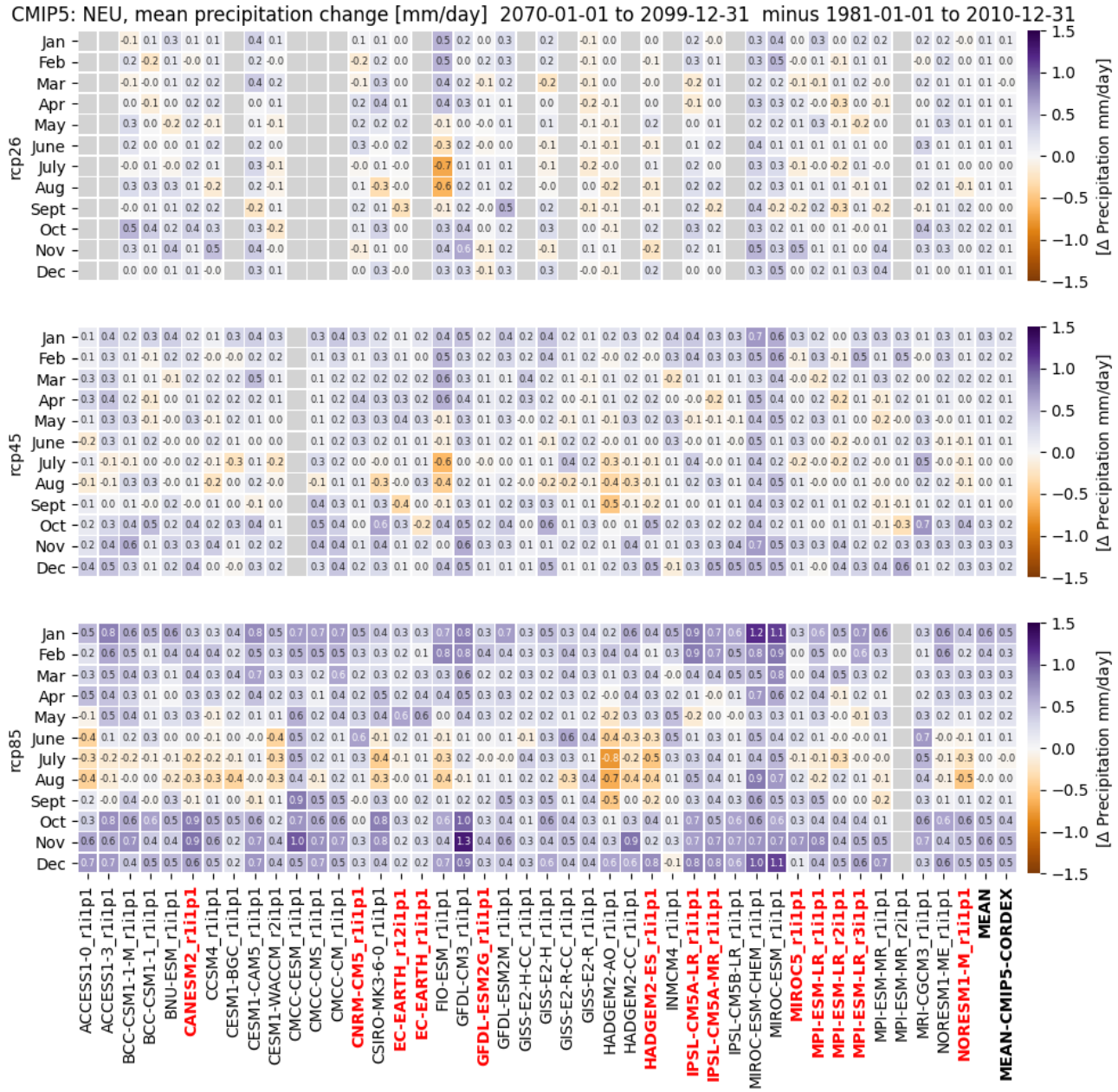

Figure A7.1. Northern Europe (NEU): 30-year mean annual cycle of precipitation change (2070 to 2099) – (1981 to 2010) calculated by the GCMs from CMIP5, the CMIP5 GCMs used as forcing for the EURO-CORDEX RCMs are highlighted in red, from top to bottom: RCP2.6, RCP4.5, RCP8.5. The boxes are grey, if a simulation was not available. The changes for each region and model are given with a number and shaded with colors according to the color bars to the right.

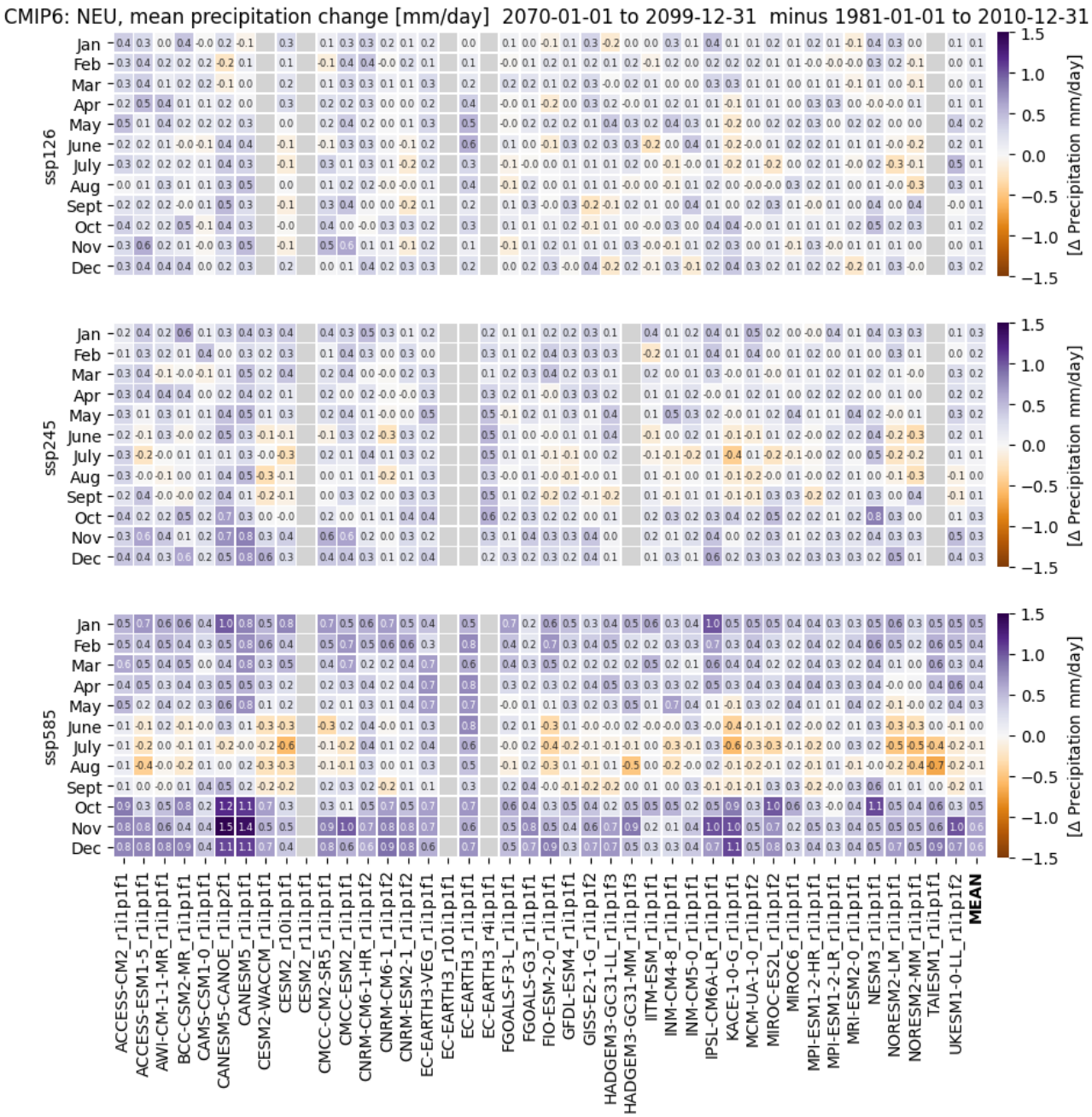

Figure A7.2. Northern Europe (NEU): 30-year mean annual cycle of precipitation change (2070 to 2099) – (1981 to 2010) calculated by the GCMs from CMIP6, from top to bottom: SSP1-2.6, SSP2-4.5, SSP5-8.5. The boxes are grey, if a simulation was not available. The changes for each region and model are given with a number and shaded with colors according to the color bars to the right.

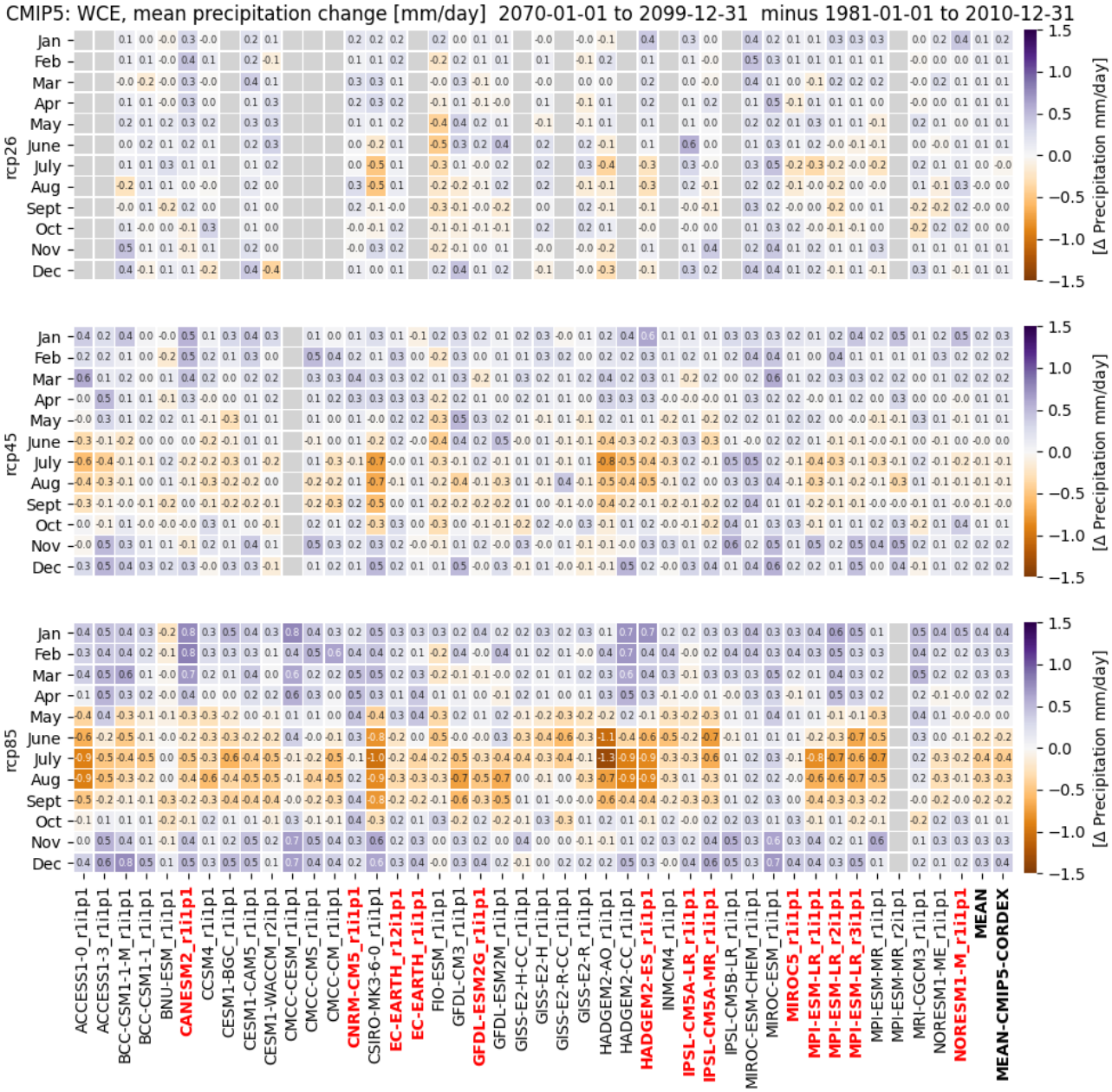

Figure A7.3. Western & Central Europe (WCE): 30-year mean annual cycle of precipitation change (2070 to 2099) – (1981 to 2010) calculated by the GCMs from CMIP5, the CMIP5 GCMs used as forcing for the EURO-CORDEX RCMs are highlighted in red, from top to bottom: RCP2.6, RCP4.5, RCP8.5. The boxes are grey, if a simulation was not available. The changes for each region and model are given with a number and shaded with colors according to the color bars to the right.

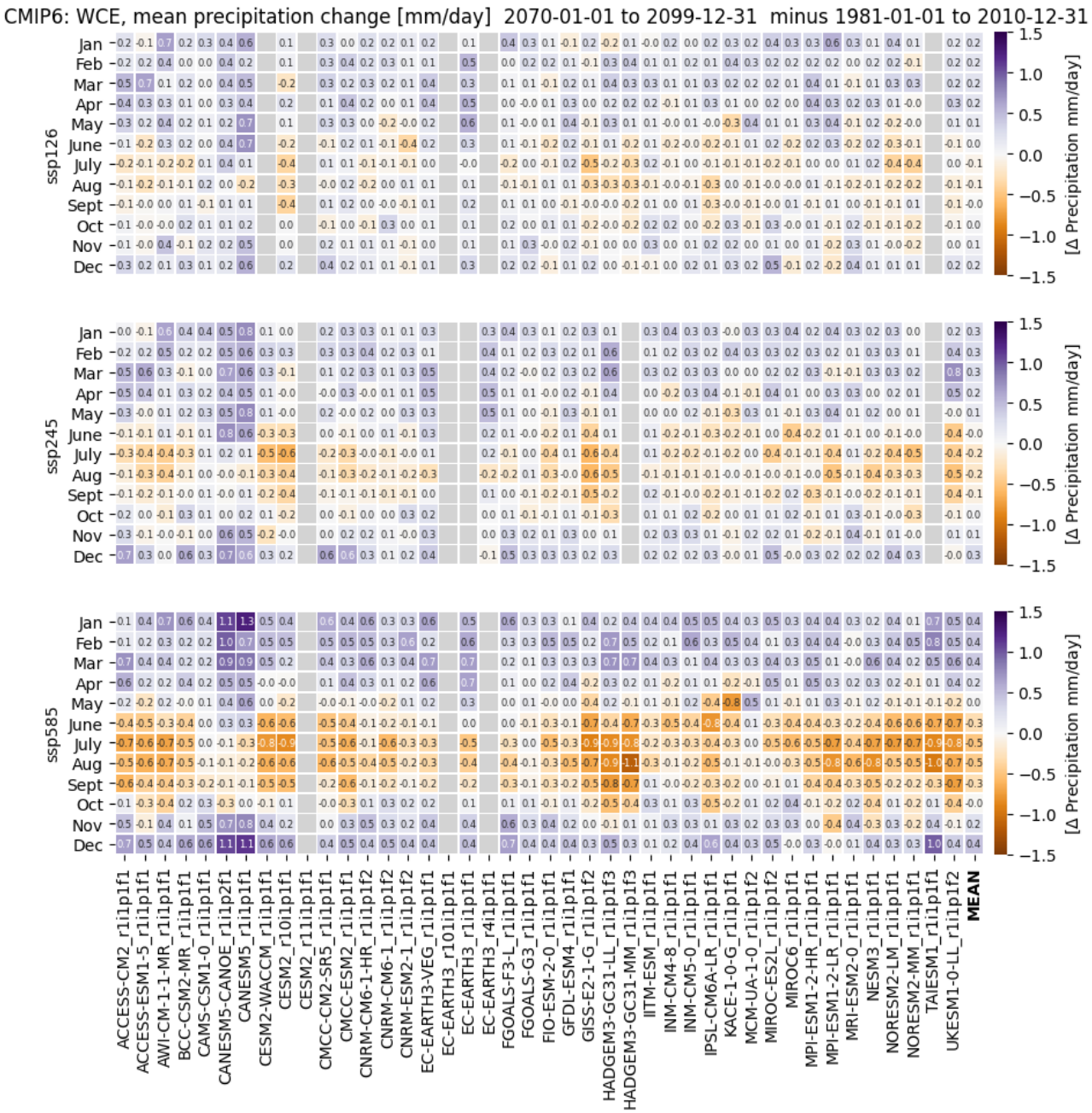

Figure A7.4. Western & Central Europe (WCE): 30-year mean annual cycle of precipitation change (2070 to 2099) – (1981 to 2010) calculated by the GCMs from CMIP6, from top to bottom: SSP1-2.6, SSP2-4.5, SSP5-8.5. The boxes are grey, if a simulation was not available. The changes for each region and model are given with a number and shaded with colors according to the color bars to the right.

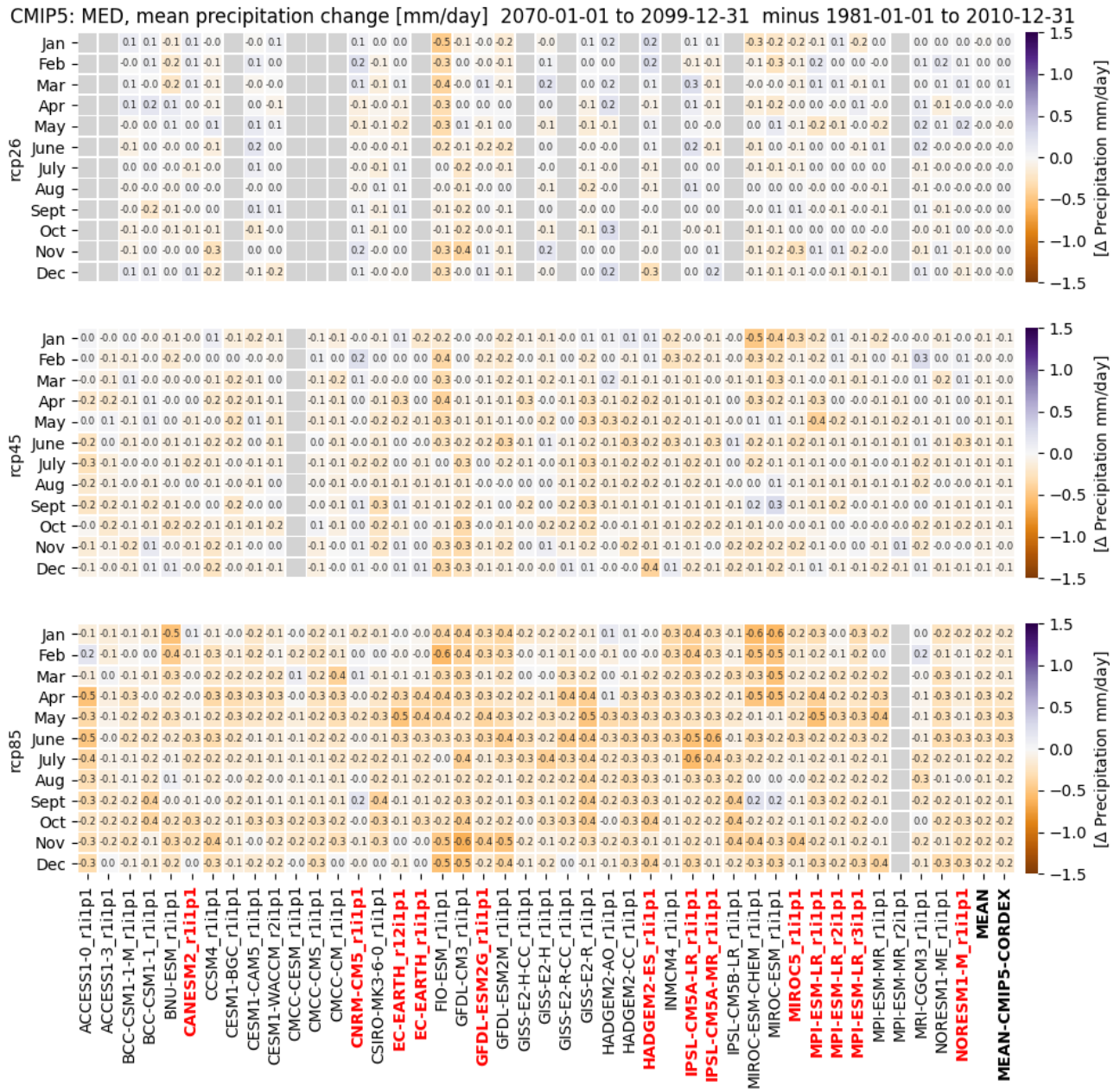

Figure A7.5. Mediterranean (MED): 30-year mean annual cycle of precipitation change (2070 to 2099) – (1981 to 2010) calculated by the GCMs from CMIP5, the CMIP5 GCMs used as forcing for the EURO-CORDEX RCMs are highlighted in red, from top to bottom: RCP2.6, RCP4.5, RCP8.5. The boxes are grey, if a simulation was not available. The changes for each region and model are given with a number and shaded with colors according to the color bars to the right.

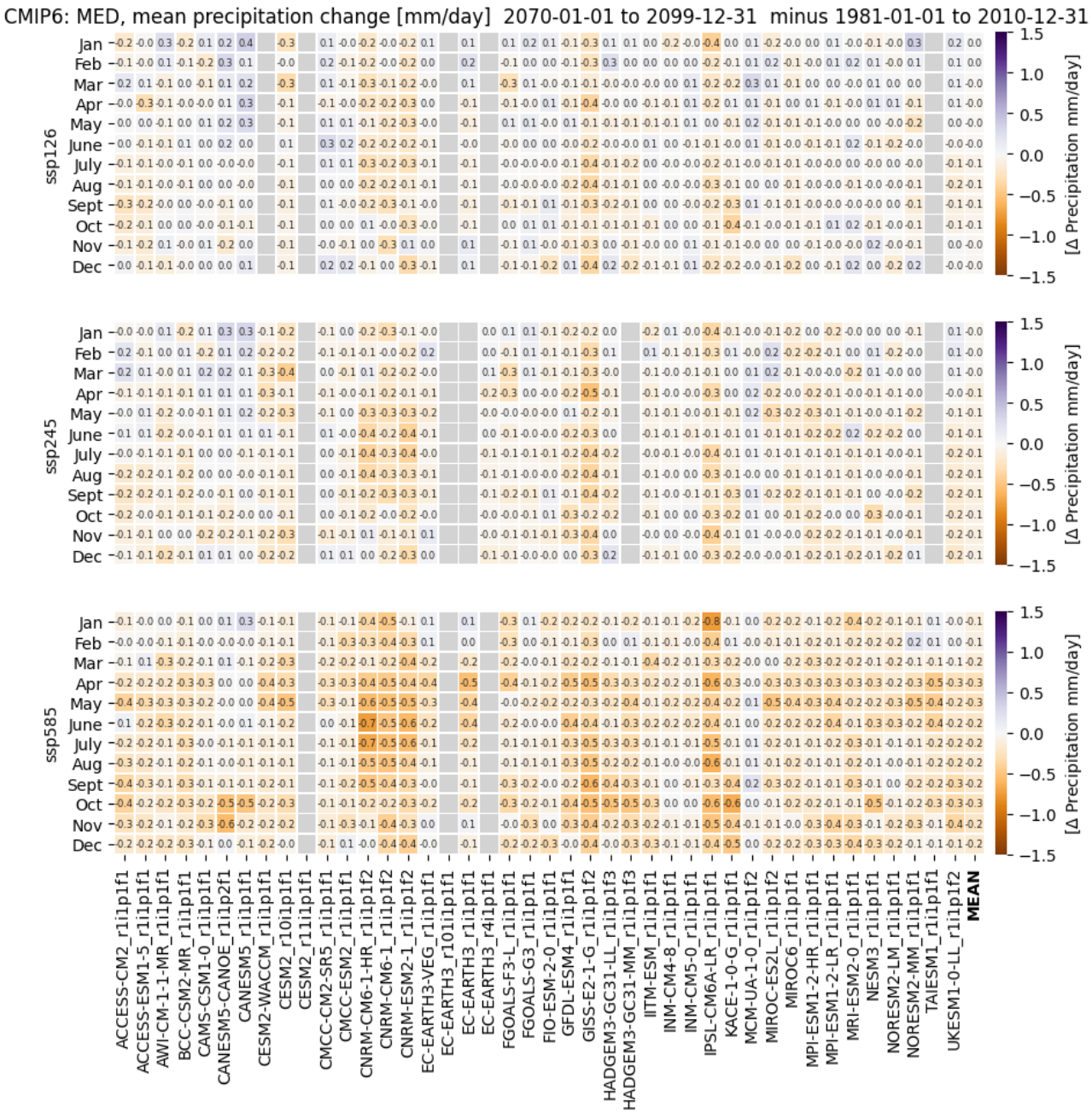

Figure A7.6. Mediterranean (MED): 30-year mean annual cycle of precipitation change (2070 to 2099) – (1981 to 2010) calculated by the GCMs from CMIP6, from top to bottom: SSP1-2.6, SSP2-4.5, SSP5-8.5. The boxes are grey, if a simulation was not available. The changes for each region and model are given with a number and shaded with colors according to the color bars to the right.

8. Annual mean precipitation and temperature change for most scenarios from CMIP5 and CMIP6

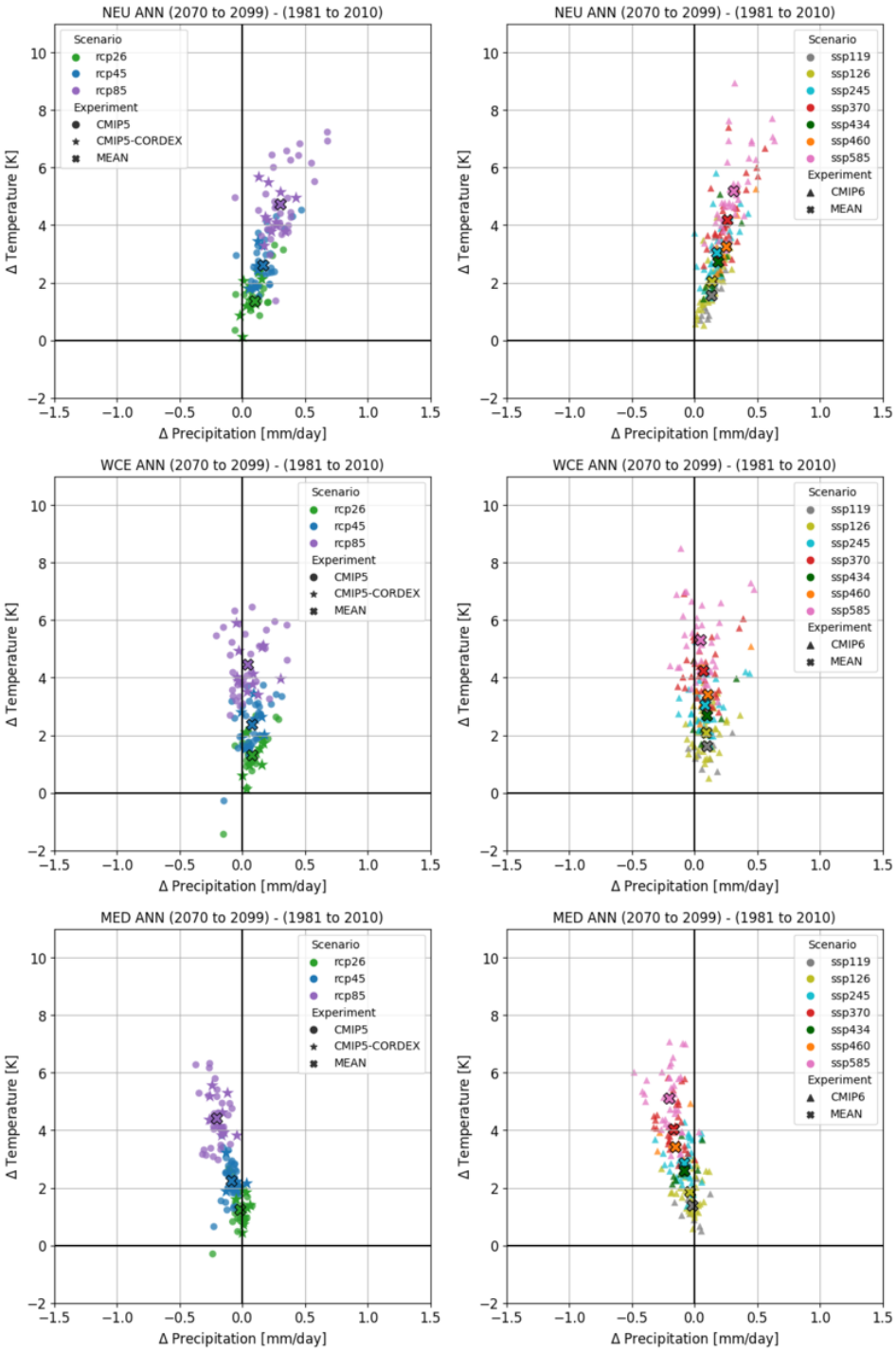

Figure A8. 30-year mean annual temperature and precipitation change (2070 to 2099) – (1981 to 2010) calculated by the GCMs from CMIP5 (RCP2.6, RCP4.5, RCP8.5) and CMIP6 (SSP1-1.9, SSP1-2.6, SSP2-4.5, SSP3-7.0, SSP4-3.4, SSP4-6.0, SSP5-8.5), the CMIP5 GCMs used as forcing for the EURO-CORDEX RCMs are highlighted as stars, from left to right: CMIP5, CMIP6, from top to bottom the regions: Northern Europe (NEU), Western & Central Europe (WCE) and Mediterranean (MED).

9. Lists of models

Table A9.1. CMIP5 models; Yellow highlights: downscaled by EURO-CORDEX

CMIP5		2036-2065; 2070-2099			1981-2010
Model	Realisation	RCP2.6	RCP4.5	RCP8.5	historical
ACCESS1-0	r1i1p1		x	x	x
ACCESS1-3	r1i1p1		x	x	x
BNU-ESM	r1i1p1	x	x	x	x
CCSM4	r1i1p1	x	x	x	x
CESM1-BGC	r1i1p1		x	x	x
CESM1-CAM5	r1i1p1	x	x	x	x
CESM1-WACCM	r2i1p1	x	x	x	x
CMCC-CESM	r1i1p1			x	x
CMCC-CMS	r1i1p1		x	x	x
CMCC-CM	r1i1p1		x	x	x
CNRM-CM5	r1i1p1	x	x	x	x
CSIRO-Mk3-6-0	r1i1p1	x	x	x	x
CanESM2	r1i1p1	x	x	x	x
EC-EARTH	r12i1p1	x	x	x	x
EC-EARTH	r1i1p1	x	x	x	x
FIO-ESM	r1i1p1	x	x	x	x
GFDL-CM3	r1i1p1	x	x	x	x
GFDL-ESM2G	r1i1p1	x	x	x	x
GFDL-ESM2M	r1i1p1	x	x	x	x
GISS-E2-H-CC	r1i1p1		x	x	x
GISS-E2-H	r1i1p2	x	x	x	x
GISS-E2-R-CC	r1i1p1		x	x	x
GISS-E2-R	r1i1p2	x	x	x	x
HadGEM2-AO	r1i1p1	x	x	x	x
HadGEM2-CC	r1i1p1		x	x	x
HadGEM2-ES	r1i1p1	x	x	x	x
IPSL-CM5A-LR	r1i1p1	x	x	x	x
IPSL-CM5A-MR	r1i1p1	x	x	x	x
IPSL-CM5B-LR	r1i1p1		x	x	x
MIROC-ESM-CHEM	r1i1p1	x	x	x	x
MIROC-ESM	r1i1p1	x	x	x	x
MIROC5	r1i1p1	x	x	x	x
MPI-ESM-LR	r1i1p1	x	x	x	x
MPI-ESM-LR	r2i1p1	x	x	x	x
MPI-ESM-LR	r3i1p1	x	x	x	x
MPI-ESM-MR	r1i1p1	x	x	x	x
MPI-ESM-MR	r2i1p1		x		x
MRI-CGCM3	r1i1p1	x	x	x	x
NorESM1-ME	r1i1p1	x	x	x	x
NorESM1-M	r1i1p1	x	x	x	x
bcc-csm1-1-m	r1i1p1	x	x	x	x
bcc-csm1-1	r1i1p1	x	x	x	x
inmcm4	r1i1p1		x	x	x

Table A9.2. CMIP6 models; Red: wrong values are published in the ESGF files, therefore this model is excluded from this study; green: Boundary conditions for possible RCM downscaling available.

CMIP6		2036 - 2065 and 2070 - 2099				1981-2010
Model	Realisation	SSP3-7.0	SSP5-8.5	SSP1-2.6	SSP2-4.5	historical
ACCESS-CM2	r1i1p1f1	x	x	x	x	x
ACCESS-ESM1-5	r1i1p1f1	x	x	x	x	x
AWI-CM-1-1-MR	r1i1p1f1	x	x	x	x	x
BCC-CSM2-MR	r1i1p1f1	x	x	x	x	x
CAMS-CSM1-0	r1i1p1f1	x	x	x	x	x
CESM2-WACCM	r1i1p1f1	x	x	x	x	x
CESM2	r10i1p1f1		x	x	x	x
CESM2	r11i1p1f1	x				x
CIESM	r1i1p1f1		x	x	x	x
CMCC-CM2-SR5	r1i1p1f1	x	x	x	x	x
CMCC-ESM2	r1i1p1f1		x	x	x	x
CNRM-CM6-1-HR	r1i1p1f2	x	x	x	x	x
CNRM-CM6-1	r1i1p1f2	x	x	x	x	x
CNRM-ESM2-1	r1i1p1f2	x	x	x	x	x
CNRM-ESM2-1	r2i1p1f2					x
CanESM5-CanOE	r1i1p2f1	x	x	x	x	x
CanESM5	r1i1p1f1	x	x	x	x	x
EC-Earth3-Veg	r1i1p1f1	x	x	x	x	x
EC-Earth3	r101i1p1f1					x
EC-Earth3	r1i1p1f1	x	x	x		x
EC-Earth3	r4i1p1f1					x
FGOALS-f3-L	r1i1p1f1	x	x	x	x	x
FGOALS-g3	r1i1p1f1	x	x	x	x	x
FIO-ESM-2-0	r1i1p1f1		x	x	x	x
GFDL-ESM4	r1i1p1f1		x	x	x	x
GISS-E2-1-G	r1i1p1f2	x	x	x	x	x
HadGEM3-GC31-LL	r1i1p1f3		x	x	x	x
HadGEM3-GC31-MM	r1i1p1f3		x	x		x
IITM-ESM	r1i1p1f1	x	x	x	x	x
INM-CM4-8	r1i1p1f1	x	x	x	x	x
INM-CM5-0	r1i1p1f1	x	x	x	x	x
IPSL-CM6A-LR	r1i1p1f1	x	x	x	x	x
KACE-1-0-G	r1i1p1f1	x	x	x	x	x
MCM-UA-1-0	r1i1p1f2	x	x	x	x	x
MIROC-ES2L	r1i1p1f2	x	x	x	x	x
MIROC6	r1i1p1f1	x	x	x	x	x
MPI-ESM1-2-HR	r1i1p1f1	x	x	x	x	x
MPI-ESM1-2-LR	r1i1p1f1	x	x	x	x	x
MPI-ESM-1-2-HAM	r1i1p1f1	x	x	x	x	x
MRI-ESM2-0	r1i1p1f1	x	x	x	x	x
NESM3	r1i1p1f1		x	x	x	x
NorESM2-LM	r1i1p1f1	x	x	x	x	x
NorESM2-MM	r1i1p1f1	x	x	x	x	x
TaiESM1	r1i1p1f1	x	x			x
UKESM1-0-LL	r1i1p1f2	x	x	x	x	x

Table A9.3. CMIP5 models used in the key literature

CMIP5 Model	(Harvey et al., 2020): historical, RCP4.5	(Oudar et al., 2020): historical, RCP8.5	(Tokarska et al., 2020): historical, RCP8.5	(Brands, 2021): historical	(Fabiano et al., 2021): historical, RCP8.5	(Fernandez-Granja et al., 2021)
ACCESS1-0	1	1	1	1	1	
ACCESS1-3	1	1		1	1	
BNU-ESM	1				1	
CCSM4	1	1	1	1		
CESM1-BGC	1	1				
CESM1-CAM5	1					
CESM1-WACCM	1					
CMCC-CESM					1	
CMCC-CMS	1	1			1	
CMCC-CM	1			1	1	
CMCC-CM2-SR5				1		
CNRM-CM5	1	1	1	1	1	1
CSIRO-Mk3-6-0	1	1	1			
CanESM2		1	1	1	1	1
EC-EARTH	1			1		1
FIO-ESM		1				
FGOALS-g2	1	1	1		1	
GFDL-CM3	1	1	1	1	1	
GFDL-ESM2G	1	1	1		1	
GFDL-ESM2M	1	1	1			1
GISS-E2-H-CC						
GISS-E2-H			1	1		
GISS-E2-R-CC						
GISS-E2-R	r6i1p1	1	1	1		
HadGEM2-AO						
HadGEM2-CC	1	1		1	1	
HadGEM2-ES	r2i1p1	1	1	1	1	1
IPSL-CM5A-LR	1	1	1	1	1	1
IPSL-CM5A-MR	1	1		1	1	
IPSL-CM5B-LR	1	1	1		1	
MIROC-ESM-CHEM	1	1			1	
MIROC-ESM	1	1	1	1	1	
MIROC5	1	1	1	1	1	1
MPI-ESM-LR	1	1	1	1	1	1
MPI-ESM-MR	1	1		1	1	
MPI-ESM-P					1	
MRI-CGCM3	1	1	1		1	
MRI-ESM1				1	1	
NorESM1-ME						
NorESM1-M	1	1	1		1	1
bcc-csm1-1-m	1	1	1		1	
bcc-csm1-1	1	1	1		1	
inmcm4	1	1	1	1		

Table A9.4. CMIP6 models used in the key literature

CMIP6 Model	(Harvey et al., 2020): SSP2-4.5	(Oudar et al., 2020): historical SSP5-8.5	(Tokarska et al., 2020): historical, SSP5-8.5, SSP1-2.6	(Brands, 2021): historical	(Fabiano et al., 2021): historical, SSP5-8.5, SSP3-7.0, SSP2-4.5	(Fernandez-Granja et al., 2021)
ACCESS-CM2				1	1	
ACCESS-ESM1-5				1		
AWI-CM-1-1-LR				1		
AWI-CM-1-1-MR						
AWI-ESM-1-1-LR					1	
BCC-ESM1			1		1	
BCC-CSM2-MR	1	1	1	1	1	
CAMS-CSM1-0		1	1			
CESM2-FV2					1	
CESM2-WACCM	1	1	1		1	
CESM2-WACCM-FV2					1	
CESM2	1	1	1		1	
CIESM						
CMCC-CM2-SR5						
CMCC-ESM2						
CNRM-CM6-1-HR			1	1	1	
CNRM-CM6-1	1	1	1	1	1	1
CNRM-ESM2-1	1	1	1	1	1	
CanESM5-CanOE						
CanESM5	1		1		1	1
E3SM-1-0			1			
EC-Earth3-Veg-LR				1		
EC-Earth3-Veg	1	1	1	1		
EC-Earth3		1	1	1	1	1
FGOALS-f3-L			1		1	
FGOALS-g3		1			1	
FIO-ESM-2-0						
GFDL-CM4	1	1	1	1	1	
GFDL-ESM4		1	1			1
GISS-E2-1-G			1	1	1	
GISS-E2-1-H			1		1	
HadGEM3-GC31-LL	1		1		1	
HadGEM3-GC31-MM				1	1	
IITM-ESM						
INM-CM4-8		1	1		1	
INM-CM5-0		1	1		1	
IPSL-CM6A-LR	1	1	1	1	1	1
KACE-1-0-G					1	
MCM-UA-1-0		1				
MIROC-ES2L		1	1	1		
MIROC6		1	1	1	1	1
MPI-ESM1-2-HR		1	1	1	1	
MPI-ESM1-2-LR				1	1	1
MPI-ESM-1-2-HAM				1	1	
MRI-ESM2-0	1	1	1	1	1	
NESM3		1	1	1		
NorCPM1			1			

NorESM1-M				1		
NorESM2-LM			1	1	1	1
NorESM2-MM				1	1	
SAM0-UNICON			1	1		
TaiESM1					1	
UKESM1-0-LL	1	1	1		1	1

10. References

Brands, S.: A circulation-based performance atlas of the CMIP5 and 6 models for regional climate studies in the northern hemisphere, Geosci. Model Dev. Discuss., (February), 1–48, doi:10.5194/gmd-2020-418, 2021.

Fabiano, F., Meccia, V. L., Davini, P., Ghinassi, P. and Corti, S.: A regime view of future atmospheric circulation changes in northern mid-latitudes, Weather Clim. Dyn., 2(1), 163–180, doi:10.5194/wcd-2-163-2021, 2021.

Fernandez-Granja, J. A., Casanueva, A., Bedia, J. and Fernandez, J.: Improved atmospheric circulation over Europe by the new generation of CMIP6 earth system models, Clim. Dyn., doi:10.1007/s00382-021-05652-9, 2021.

Harvey, B. J., Cook, P., Shaffrey, L. C. and Schiemann, R.: The Response of the Northern Hemisphere Storm Tracks and Jet Streams to Climate Change in the CMIP3, CMIP5, and CMIP6 Climate Models, J. Geophys. Res. Atmos., 125(23), 1–10, doi:10.1029/2020JD032701, 2020.

Iturbide, M., Gutiérrez, J. M., Alves, L. M., Bedia, J., Cimadevilla, E., Cofiño, A., Cerezo-Mota, R., Di Luca, A., Faria, S. H., Gorodetskaya, I., Hauser, M., Herrera, S., Hewitt, H., Hennessy, K., Jones, R., Krakovska, S., Manzanas, R., Marínez-Castro, D., Narisma, G. T., Nurhati, I., Pinto, I., Seneviratne, S., van den Hurk, B. and Vera, C.: An update of IPCC climate reference regions for subcontinental analysis of climate model data: Definition and aggregated datasets, Earth Syst. Sci. Data Discuss., (January), 1–16, doi:10.5194/essd-2019-258, 2020.

Meinshausen, M., Smith, S. J., Calvin, K., Daniel, J. S., Kainuma, M. L. T., Lamarque, J., Matsumoto, K., Montzka, S. A., Raper, S. C. B., Riahi, K., Thomson, A., Velders, G. J. M. and van Vuuren, D. P. P.: The RCP greenhouse gas concentrations and their extensions from 1765 to 2300, Clim. Change, 109(1), 213–241, doi:10.1007/s10584-011-0156-z, 2011.

Meinshausen, M., Nicholls, Z. R. J., Lewis, J., Gidden, M. J., Vogel, E., Freund, M., Beyerle, U., Gessner, C., Nauels, A., Bauer, N., Canadell, J. G., Daniel, J. S., John, A., Krummel, P. B., Luderer, G., Meinshausen, N., Montzka, S. A., Rayner, P. J., Reimann, S., Smith, S. J., Van Den Berg, M., Velders, G. J. M., Vollmer, M. K. and Wang, R. H. J.: The shared socio-economic pathway (SSP) greenhouse gas concentrations and their extensions to 2500, Geosci. Model Dev., 13(8), 3571–3605, doi:10.5194/gmd-13-3571-2020, 2020.

Oudar, T., Cattiaux, J. and Douville, H.: Drivers of the Northern Extratropical Eddy-Driven Jet Change in CMIP5 and CMIP6 Models, Geophys. Res. Lett., 47(8), 1–9, doi:10.1029/2019GL086695, 2020.

Tebaldi, C., Debeire, K., Eyring, V., Fischer, E., Fyfe, J., Friedlingstein, P., Knutti, R., Lowe, J., O'Neill, B., Sanderson, B., Van Vuuren, D., Riahi, K., Meinshausen, M., Nicholls, Z., Tokarska, K., Hurtt, G., Kriegler, E., Meehl, G., Moss, R., Bauer, S., Boucher, O., Brovkin, V., Yhb, Y., Dix, M., Gualdi, S., Guo, H., John, J., Kharin, S., Kim, Y. H., Koshiro, T., Ma, L., Olivié, D., Panickal, S., Qiao, F., Rong, X., Rosenbloom, N., Schupfner, M., Séférian, R., Sellar, A., Semmler, T., Shi, X., Song, Z., Steger, C., Stouffer, R., Swart, N., Tachiiri, K., Tang, Q., Tatebe, H., Voldoire, A., Volodin, E., Wyser, K., Xin, X., Yang, S., Yu, Y. and Ziehn, T.: Climate model projections from the Scenario Model Intercomparison Project (ScenarioMIP) of CMIP6, Earth Syst. Dyn., 12(1), 253–293, doi:10.5194/esd-12-253-2021, 2021.

Tokarska, K. B., Stolpe, M. B., Sippel, S., Fischer, E. M., Smith, C. J., Lehner, F. and Knutti, R.: Past warming trend constrains future warming in CMIP6 models, Sci. Adv., 6(12), 1–14, doi:10.1126/sciadv.aaz9549, 2020.

ECMWF - Shinfield Park, Reading RG2 9AX,
UK

Contact: info@copernicus-climate.eu

climate.copernicus.eu copernicus.eu